Received: 11 August 2022 | Revised: 28 October 2022 | Accepted: 1 November 2022

DOI: 10.1002/dvdy.551

RESEARCH ARTICLE

Developmental Dynamics WILEY

A comparative analysis of the ontogeny of syngnathids (pipefishes and seahorses) reveals how heterochrony contributed to their diversification

Ralf F. Schneider[1,2] | **Joost M. Woltering**[3] | **Dominique Adriaens**[4] | **Olivia Roth**[1,2]

[1]Department of Zoology, Marine Evolutionary Biology, University of Kiel, Kiel, Germany

[2]Department of Marine Evolutionary Ecology, Helmholtz Centre for Ocean Research, Kiel, Germany

[3]Department of Evolutionary Biology, University of Konstanz, Konstanz, Germany

[4]Department of Biology, Ghent University, Ghent, Belgium

Correspondence
Ralf F. Schneider, Department of Zoology, Marine Evolutionary Biology, University of Kiel, Kiel, Germany.
Email: rschneider@zoologie.uni-kiel.de

Funding information
Deutsche Forschungsgemeinschaft, Grant/Award Numbers: WO-2165/2-1, WO-2165/2-2; H2020 European Research Council, Grant/Award Number: 755659

Abstract

Background: Syngnathids are a highly derived and diverse fish clade comprising the pipefishes, pipe-horses, and seahorses. They are characterized by a plethora of iconic traits that increasingly capture the attention of biologists, including geneticists, ecologists, and developmental biologists. The current understanding of the origins of their derived body plan is, however, hampered by incomplete and limited descriptions of the early syngnathid ontogeny.

Results: We provide a comprehensive description of the development of *Nerophis ophidion*, *Syngnathus typhle*, and *Hippocampus erectus* from early cleavage stages to release from the male brooding organ and beyond, including juvenile development. We comparatively describe skeletogenesis with a particular focus on dermal bony plates, the snout-like jaw morphology, and appendages.

Conclusions: This most comprehensive and detailed account of syngnathid development to date suggests that convergent phenotypes (e.g., reduction and loss of the caudal fins), likely arose by distinct ontogenetic means in pipefishes and seahorses. Comparison of the ontogenetic trajectories of *S. typhle* and *H. erectus* provides indications that characteristic features of the seahorse body plan result from developmental truncation. Altogether, this work provides a valuable resource and framework for future research to understand the evolution of the outlandish syngnathid morphology from a developmental perspective.

KEYWORDS
bone, cartilage, development, morphology, pipefish, seahorse, teleost

1 | INTRODUCTION

Syngnathids (pipefishes, pipe-horses and seahorses) are a globally distributed taxon of highly derived fishes that evolved a plethora of bizarre and unique phenotypes. Examples are the elongated, fin-reduced bodies of the pipefishes,[1] the leaf-mimicking appendages of the leafy seadragons,[2,3] the curved body posture that permits upright swimming in seahorses,[4] and of course male pregnancy—a unique trait shared amongst

syngnathids.[5,6] These and other outlandish novelties of the syngnathid lineage attract an ever-increasing scientific attention.[7,8] For instance, recent studies addressed how the syngnathids' tube-like jaws and angled head posture facilitate pivot feeding,[9,10] or investigate the mechanical basis for the flexible and strong prehensile tail.[11,12] A full comprehension of the evolutionary history of lineage specific morphological novelties, that is beyond their adaptive significance or adult physiology, requires knowledge of how these traits form during embryonic development. In case of the syngnathids, several factors complicate the study of their ontogeny. First, laboratory work on syngnathids requires a dedicated marine facility and breeding only occurs with optimized husbandry. Alternatively, embryonic material can be collected in the field but typically this is cumbersome with respect to culturing and documentation. Second, syngnathids have a reproductive strategy involving paternal care: during mating, the female's ovipositor transfers the unfertilized eggs to the male by either attaching them to open brooding patches (less derived species) or depositing them into the male's brooding pouch (more derived species), where eggs are subsequently fertilized and develop until embryos are released.[13] Especially in species with more derived brooding pouches the developmental stage of an embryo can typically only be observed after dissecting the father and obtained embryos often cannot be cultured outside of the specific microenvironment provided by the brooding organ, which further complicates studies of embryonic development. Additionally, many syngnathids (e.g., seahorses and *Syngnathus* pipefishes) produce embryos that upon release already possess the adult body plan and thus do not pass through a specialized free-living larval stage—that is, they qualify as direct developers.[14-16] Therefore, the most informative developmental stages need to be collected from the brooding organ through more or less invasive procedures (depending on the species and type of brooding organ, see below). Thus, to study the developmental biology of specific morphological features, such as the elongated snout or fin loss in pipefishes, their prerelease development must be considered.

Syngnathid embryonic and juvenile development has been the subject of several studies: Novelli et al[17,18] provided a detailed description of the chondro- and osteoskeletal development in juvenile Short-snouted seahorses (*Hippocampus hippocampus)* throughout the first month post-release and of the inner organs in juvenile Longsnout seahorses (*Hippocampus reidi*), confirming that loss of the (functional) spleen is an adult phenomenon. Franz-Odendaal et al[19] focused on post-release development of the juvenile seahorses' head skeleton proposing that heterochronic shifts contribute to interspecific differences in head morphology. Studies investigating prerelease (i.e., embryonic) development are scarcer, and often rely upon incidental sampling with few replications, which limits the level of detail they provide (e.g., [20-24] but see Reference 25 for approximately the second half of prerelease development, and Reference 26 for *Syngnathus* kidney development). The only comparative study spanning the entire syngnathid prerelease development we are aware of describes and compares Straightnose pipefish (*Nerophis ophidion*), Black-striped pipefish (*Syngnathus abaster*), and Big-belly seahorse (*Hippocampus abdominalis*).[21] Yet, only few developmental stages per species are described and developmental timing is estimated according to previous studies on related species. Furthermore, the study by Azzarello[25] focuses on the second half of prerelease development. However, due to its publication in 1990, the quality of images provided is limited to the standards of the time. Therefore, a comprehensive comparative study describing and illustrating syngnathid development remains a timely contribution to the field.

Here, we comparatively described the prerelease development of representatives of three deep syngnathid branches (Figure 1A), the *Nerophinae* (52 species recognized[27]; represented by the Straightnose pipefish, *N. ophidion*; Figure 1B), *Syngnathinae* (253 species recognized incl. *Hippocampinae*[27]; represented by the Broadnose pipefish, *Syngnathus typhle*; Figure 1C), and *Hippocampinae* (56 species recognized[27]; a taxon nested within the *Syngnathinae* [Figure 1A]; represented by the lined seahorse, *Hippocampus erectus*; [Figure 1D]).[28-30] More information on the early development of these species is particularly desirable as they are among the most studied syngnathids of their respective clades, long-read genomes have either already been published or are currently prepared, and selected species can be bred in captivity with relative ease, which is crucial for studies of the early development.[31] Furthermore, the fish feature an abundance of distinct morphological phenotypes and different variations of male parental care/pregnancy—the unique reproductive strategies of syngnathids (Figure 1E-G). We focus on the prerelease development and add details on post-release development for some characters. Finally, we discuss the scientific value of the syngnathid model system in the context of evo-devo research.

2 | RESULTS

2.1 | Adult morphology and breeding biology: A brief overview

The three selected syngnathid species examined in this study represent three deep branches within the

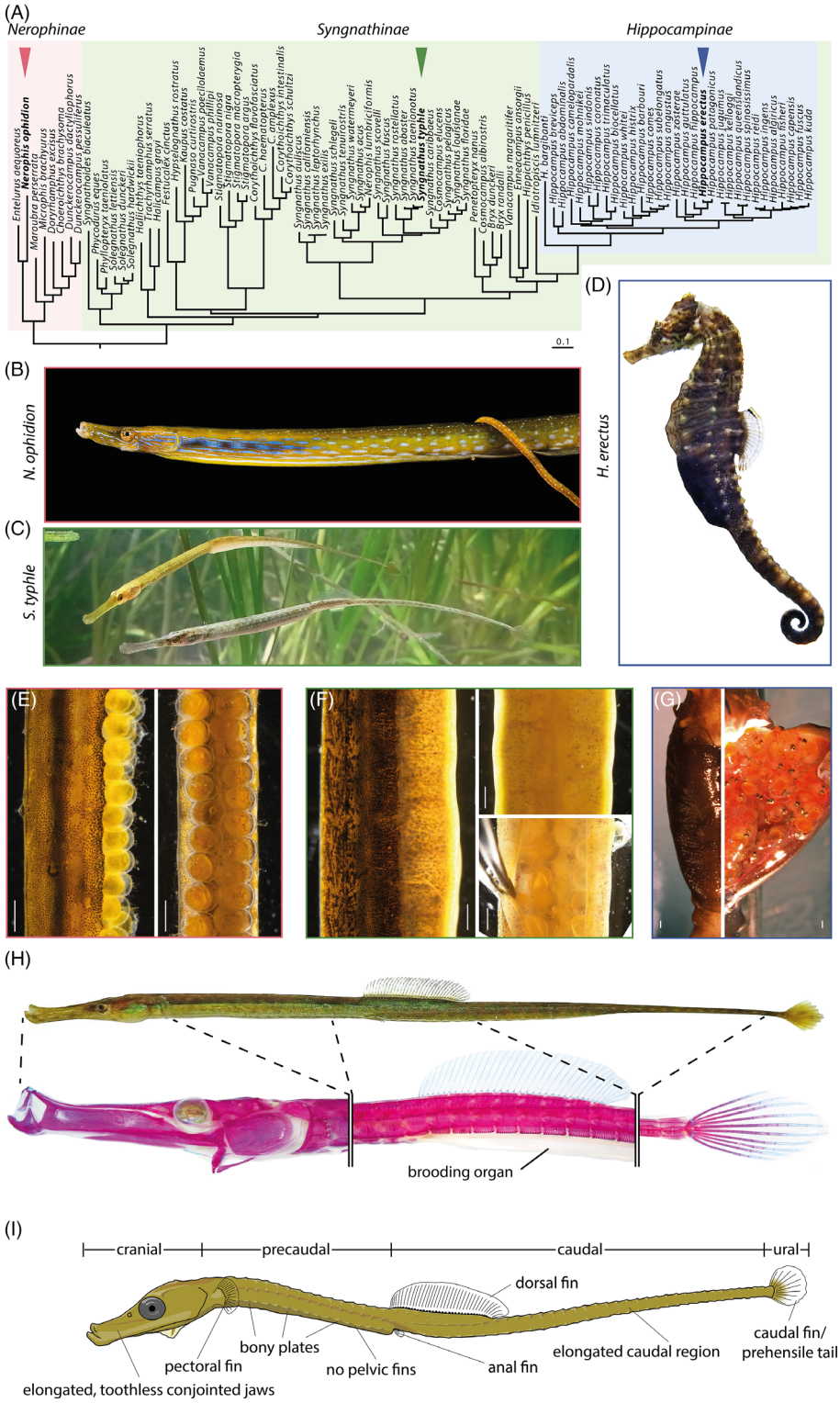

FIGURE 1 Habitus, brooding organs, and body plan of examined species. (A) Phylogenetic tree of the *Syngnathidae* family ("syngnathids") with focal clades and study species indicated.[30] (B-D) Female *Nerophis ophidion*, male (upper) and female (lower) *Syngnathus typhle*, and male *Hippocampus erectus*, respectively. (E) Male *N. ophidion* brooding organ with eggs located along the animals' trunk (left: lateral view; right: ventral view). (F) Male *S. typhle* brooding organs are on the animal's tail and cover the eggs (left: lateral view; upper right: ventral view; lower right: ventral view with covering skin pulled aside). (G) Male *H. erectus* carry the developing embryos in a pouch-like brooding organ, which has a small anterior opening, on their tail (left: ventral view; right: ventral view with surgically opened brooding organ). (H) An Alizarin red (stains ossified tissue) and Alcian blue (stains cartilage) stain of an adult male *S. typhle* illustrates the bony armor of adult syngnathids. (I) Schematic drawing of a *S. typhle* juvenile featuring syngnathid traits focal for this study. Photo in (D) by Uli Kunz

syngnathids radiation (Figure 1A), and display many of their diverse phenotypes (Figure 1).[28] The straightnose pipefish (*N. ophidion*) is a primarily European species with a preference for brackish water. It has an extremely thin and elongated body (33 precaudal and 73 caudal vertebrae; Table 1), with males typically being approximately 20 cm long (with a maximum body diameter of 3-4 mm) while the females are larger and can reach lengths of approximately 30 cm (with a maximum body diameter of 4-6 mm, not accounting for an ornamental ventral longitudinal skin protrusion[32]; Figure 1B). Adult *N. ophidion* have only a dorsal fin, which contains 33 soft-rays (Table 1). Note that all syngnathids lack the fin spines present in other spiny-rayed fishes as a result

TABLE 1 Adults' vertebrae and ray numbers observed in studied species

	Nerophis ophidion	*Syngnathus typhle*	*Hippocampus erectus*
Precaudal vertebrae	33	19	12
Caudal vertebrae	73	36	35
Ural vertebrae	0	1	1
Pectoral fin rays	NA	14	16
Dorsal fin rays	33	37	18
Anal fin rays	NA	3	4
Caudal fin rays	NA	10	0 (2–5 rud.)

of secondary loss.[33] The posterior body axis does not terminate in a caudal fin but instead forms a (semi-)prehensile tail used by the fish to wrap themselves around holdfasts, such as eelgrass.[34] Females have a membrane ventrolateral along their trunk that is erected during intraspecific interactions. For syngnathids, *N. ophidion* has a relatively small head and short snout (Figure 1B).

The broadnose pipefish (*S. typhle*) is also a European species. It has a less extremely elongated body (with 19 precaudal, 36 caudal and one ural vertebra) and males and females are more equal in size, with both rarely reaching substantially over 20 cm in our sampling area of the Baltic Sea (with a maximum body diameter of approximately 1.5 cm in nonpregnant males and nongravid females[32,35]; Figure 1C). *S. typhle* has relatively well-developed pectoral (14 rays), dorsal (37 rays), anal (3 rays), and caudal (10 rays) fins (pelvic fins are absent in all syngnathids as the result of loss of the *tbx4* gene [-Table 1]).[1,8] *S. typhle* has the long tubular snout typical for syngnathids, which in this species appears laterally compressed when compared to other pipefish species.[34] Furthermore, males have modified bony body plates with ventrolateral protrusions on the anterior portion of their tail that support the elaborate pouch-like brooding organ (Figure 1H).

The Lined seahorse (*H. erectus*) belongs to the subfamily of *Hippocampinae*, which have evolved an upright swimming posture, a prehensile muscular tail and the most derived form of pregnancy among syngnathids (Figure 1D).[36] Males and females are similar in size; approximately 6 to 12 cm with uncoiled tail.[37] However, large males typically have a deeper body due to a ventral bony trunk keel that females lack. Males also have a sealable brood pouch at the more cranial portion of their tail (Figure 1D). Their head (excluding snout) appears axially compressed when compared to other syngnathids (see also Reference 10).

N. ophidion, *S. typhle*, and *H. erectus* represent three main types of brooding organs that evolved in Syngnathids.[6] *N. ophidion* has the simplest type of brooding organ, possibly representing the ancestral state for syngnathids, which runs as a ventral abdominal groove along the ventral side of the trunk (i.e., precaudal region). The round eggs (typically 0.8-1 mm in diameter; see also Reference 32) are attached to this groove in several rows during mating (Figure 1E). Egg numbers are linked to male and female body size, but often exceed 100. On occasion, clutches are (partially) unfertilized, leading to a rejection of the unfertilized eggs after several days. Eggs found on wild-caught specimens are often overgrown by different types of algae and even small mussels are regularly found settling on the eggs. This does not seem to affect the survival of the eggs though (personal observation). Eggs are held in place by being partially engulfed by the hypertrophic brooding organ tissue.[34] The larvae are released by hatching from the egg chorion after approximately 27 days post mating (dpm; at 16°C) and remaining eggshells are discarded by the male brooding organ several hours later, when the brooding organ tissue undergoes hypotrophy.

The brooding organ of *S. typhle* evolved into a more derived, partially sealable brood pouch, which runs along the ventral side of the anterior tail (Figure 1F). In contrast to *N. ophidion*, the brooding tissue includes two muscular skin flaps running along each side of the brooding patch parallel to the body axis, which together form a pouch when closed. Outside of the mating season, these are hypotrophic and folded flat toward each other. However, when male individuals become ready to mate, these skin flaps undergo remodeling and hypertrophy, and, together with the actual brooding patch, form a U-shaped brooding unit into which the female transfers her round eggs (~1.5-2 mm in diameter; see also Reference 32). Egg numbers are smaller compared to *N. ophidion* (but still can exceed 100 in large individuals[35]), and a filled brood pouch typically holds several dozens of eggs (depending on the male size). Occasionally, only partially filled pouches are found, possibly because mates assessed their partner's attractiveness during mating as too low to invest the maximal possible number of eggs/pouch space into

the brood.[38] After mating, the male closes the brood pouch via the muscular skin flaps, which fold toward each other and cover the eggs completely. The inner endometrium-like skin of the brooding patch ("pseudo-placenta") and skin flaps then engulf the eggs almost completely. The male may mate again, typically by opening the anterior part of his brooding pouch and eggs are deposited anterior to the previous clutch.[35] *S. typhle* embryos hatch within this brooding pouch after approximately 16 dpm (at 16°C) and are released after approximately 31 dpm. Therefore, the primary difference between the brood structures of the two pipefishes investigated is that *N. ophidion* possesses an exposed brood patch whereas *S. typhle* provides a more shielded incubation environment offering increased opportunities for parental provisioning through interaction with an endometrium-like tissue.

The brooding organ of *H. erectus* is the most derived type found in syngnathids (Figure 1G). In contrast to *S. typhle*, the two skin flaps become fused at the midline during brooding organ development,[39] forming a sack-like pouch with only a small, muscular opening at the cranial end of the tail. Pear-shaped eggs (approx. 1.5 mm wide and 2.5 mm long) are deposited during mating into this pouch, where they are fertilized and engulfed by the hypertrophic endometrium-like tissue. Egg numbers again depend on male and female body sizes and range from <100 to >1500 in the wild.[37] Embryonic development commences inside the egg but embryos often hatch well before being released: we observed that in clutches of similarly developed embryos, some hatched as early as 6 dpm in the pouch while others had not yet hatched at 12 dpm, suggesting that hatching may be influence by additional factors, such as the microenvironment in the pouch or the genetic makeup of the specific embryo, rather than being ontogenetically synchronous. After 16 dpm juveniles were released from the paternal pouch (at 23°C), whereby some heterogeneity in juvenile developmental stages can be observed between batches.

2.1.1 | Prerelease development as revealed by microscopy

Prerelease development was documented using microscopy after extraction of embryos from egg-bearing males of *N. ophidion*, *S. typhle*, and *H. erectus*. Figure 2 provides an overview of the timed appearance of benchmark morphological features. Our description of prerelease development is intended as a comparative, yet global overview of syngnathid ontogeny and is arguably more limited in detail concerning morphology and developmental timing than staging series published for model species (e.g., zebrafish, medaka[40-42]). As in previous studies, the difficulties in obtaining syngnathid embryos combined with the fact that developmental speed among and within batches can vary somewhat (as reported before) made obtaining targeted stages challenging. Thus, references to developmental time should be treated as approximations (e.g., 10 dpm may mean anything from 9 dpm + 12 hours to 10 dpm + 12 hours; see Section 5 for more details). As *H. erectus* embryos were raised at higher temperatures than those of the pipefish species, prerelease development is naturally expected to be concluded faster than in species raised at lower temperature, as temperature affects developmental speed (see Section 5).

Previous literature divided syngnathid prerelease (or "prenatal") development into varying stages,[21] but the description provided here will follow these only loosely (but see Figure 2). Rather, we refer to developmental events and when these occur in the three considered species (in days post mating, or relative developmental time in percentage) as recognizing comparable developmental stages is quite subjective (as discussed in Reference 25). We adhere to terminology for "direct" and "indirect" developing species as used in References 14-16. Herein, the term "larva" is reserved for the first free feeding (i.e., postembryonic) stage, but only in cases where important differences with the adult body plan exist that only disappear upon metamorphosis, as is the case for the indirect developing *N. ophidion*. We consider *H. erectus* and *S. typhle* direct developing species in which the embryo directly transforms into a feeding juvenile, as defined by the presence of an adult-like body plan.

In our description of syngnathid ontogeny we first present the overall pre-hatch/prerelease development (early: zygote to segmentation; middle: segmentation and early organogenesis; late: organogenesis to release) while focusing on characteristics recognizable without further staining. Subsequently, a more detailed description of skeletogenesis is provided based on stained samples. Furthermore, in situ hybridization was used to explore early osteogenesis and myogenesis.

2.1.2 | Early prerelease development: From zygote to segmentation

The first third of development in all three studied syngnathid species is similar and synchronized with respect to relative developmental time (Figure 2; Figure 3): in the first days after mating (zygote, blastula, and segmentation stage), all embryos pass through the typical stages of early teleost development, including cleavage (with high, oblong, dome stage, and onset of epiboly) and gastrulation (epiboly commences, the embryonic shield forms, and the tail bud becomes visible; for reference see, for instance, zebrafish

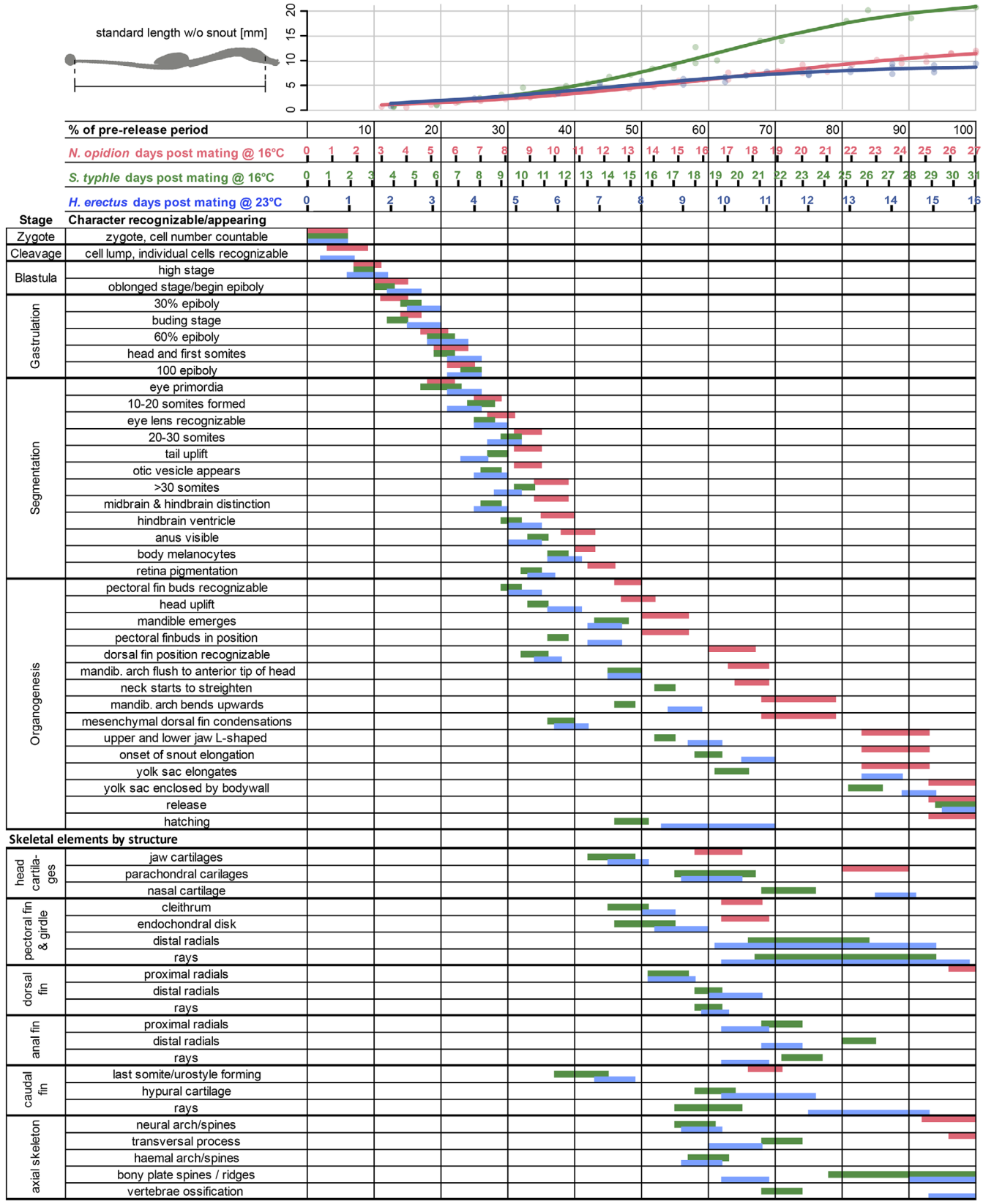

FIGURE 2 Body length and emergence sequence of syngnathid morphological characteristic during their prenatal development. Upper panel illustrates standard body length excluding snout during the prerelease development. Lines are logistic regression fit lines. Lower panel: emergence periods of morphological characteristics during the prerelease development in the three studied species *Nerophis ophidion* (red), *Syngnathus typhle* (green), and *Hippocampus erectus* (blue)

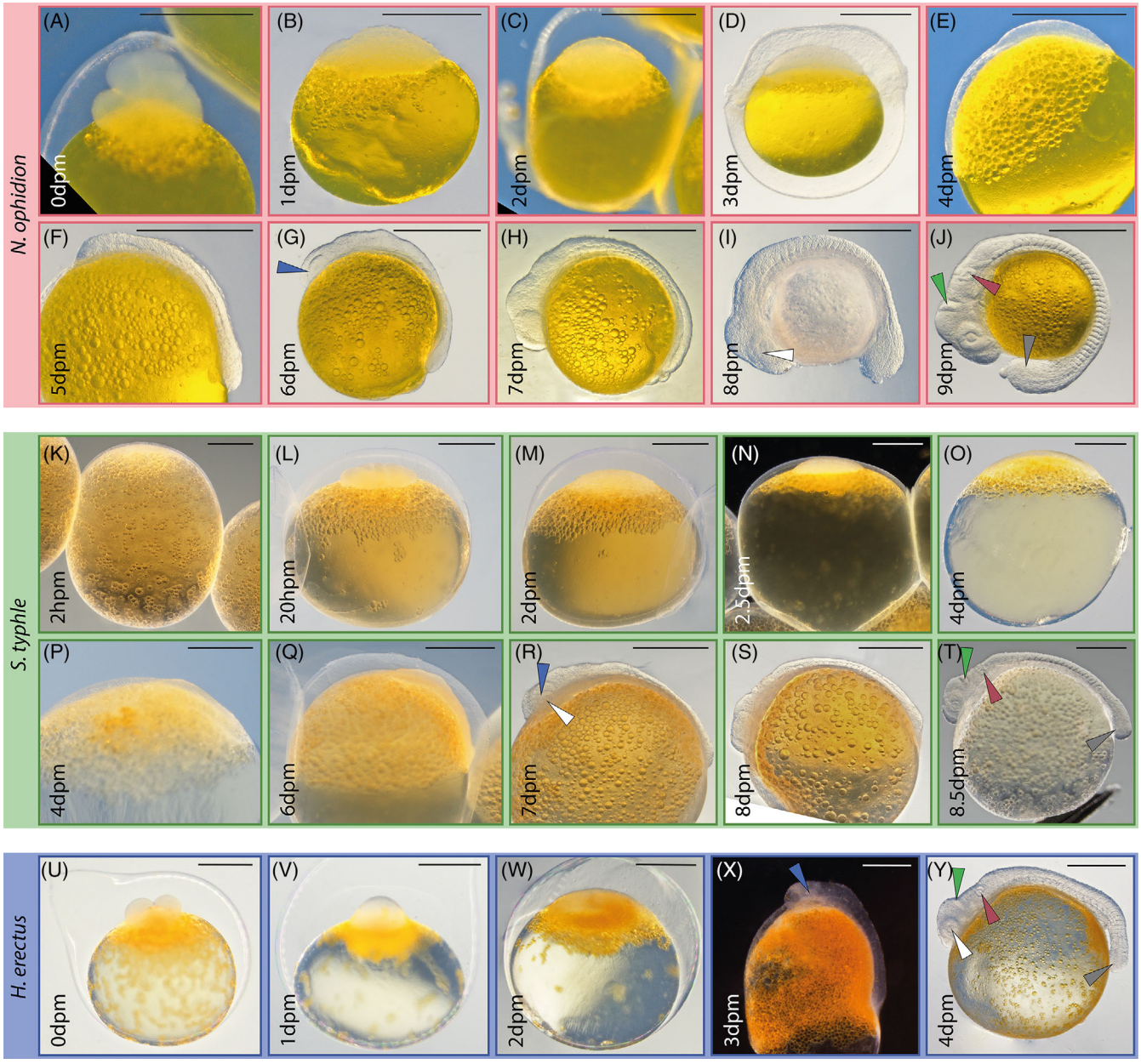

FIGURE 3 Zygote to segmentation development in examined syngnathids. *Nerophis ophidion* (A-J), *Syngnathus typhle* (K-T), and *Hippocampus erectus* (U-Y), respectively. Overall, early development is similar among studied species. Arrowheads: blue = eye cups, white = lens, purple = otic vesicle, red = otic vesicle, green = mid-hind-brain barrier, gray = tail bud. Scale is 500 μm; dpm = days post mating

staging[40]). Eye cups emerge during the segmentation stage (blue arrowheads in Figure 3G,R,X; at 6, 7, and 3 dpm in *N. ophidion*, *S. typhle*, and *H. erectus*, respectively), which is when somites become visible, and shortly after the forming lens can be observed (white arrowheads in Figure 3I,R,Y; at 8, 7, and 4 dpm in *N. ophidion*, *S. typhle*, and *H. erectus*, respectively). When the tail bud detaches from the yolk sac, mid-hindbrain barrier and the otic vesicle become visible (gray, green and purple arrowheads, respectively, in Figure 3J,T,Y; at 9, 8.5, and 4 dpm in *N. ophidion*, *S. typhle*, and *H. erectus*, respectively), *N. ophidion* embryos have completed approximately one-third of their pre-hatching development, encircle the relatively small yolk sac almost entirely, and have developed over 30 somites. In contrast, *S. typhle* reaches this stage somewhat earlier (~27% of pre-release development) but with fewer than 20 somites formed, similar to *H. erectus*, which reaches this stage approximately after 4 dpm, that is, 25% of its prerelease developmental time. The latter species' embryos also appear relatively smaller compared to yolk sac size due to the larger yolk sac. At this stage, a heartbeat was also recognizable in all species.

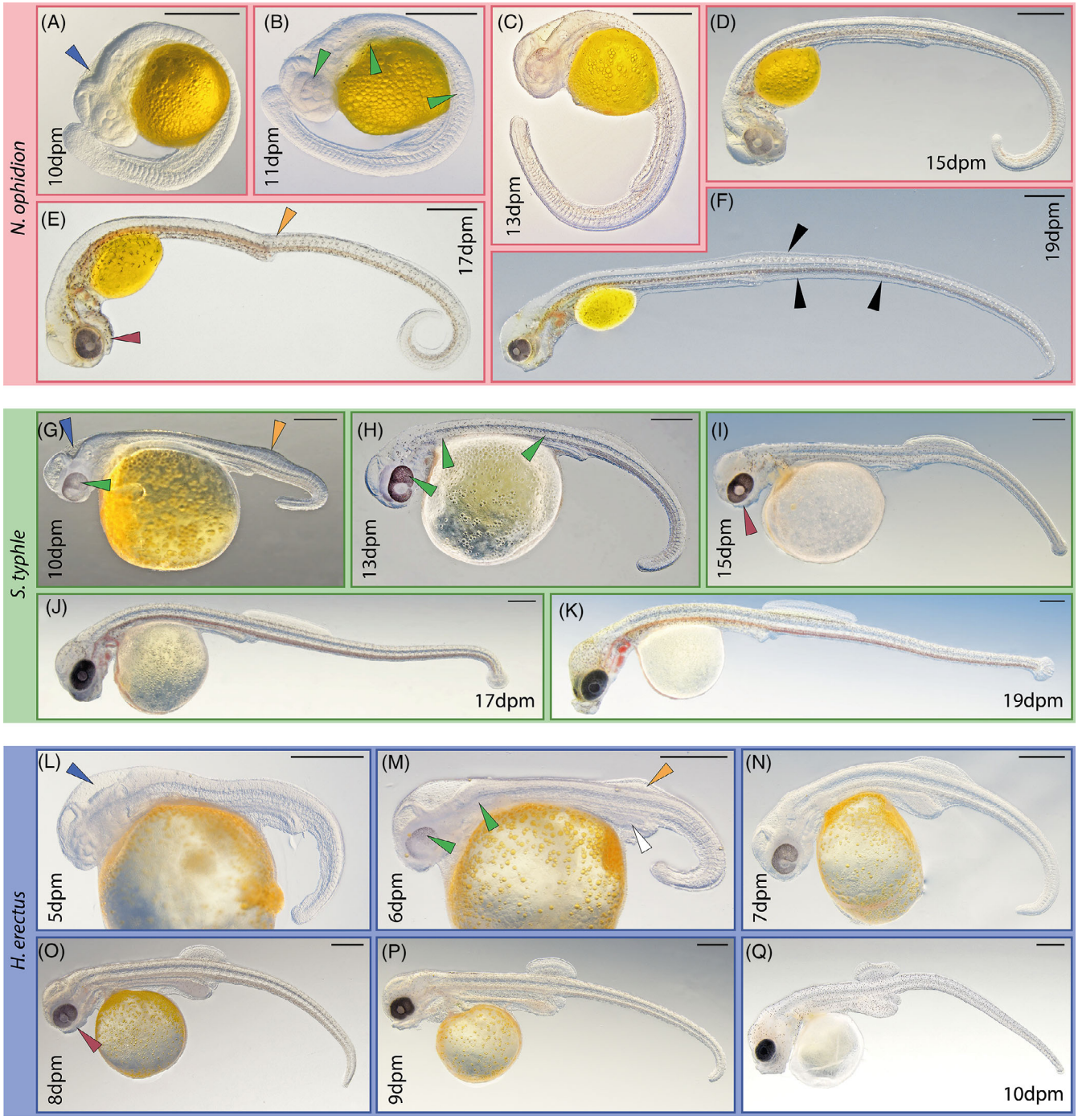

FIGURE 4 Segmentation and early organogenesis development in examined syngnathids. *Nerophis ophidion* (A-F), *Syngnathus typhle* (G-K), and *Hippocampus erectus* (L-Q), respectively. In this period, species-specific characteristics develop more clearly. Arrowheads: blue = hind brain vesicle, green = pigmentation, rufous = mandibular arch, orange = dorsal fin condensations, white = hypertrophic hindgut, black = fin fold. Scale is 500 μm; dpm = days post mating

2.1.3 | Mid prerelease development: Segmentation and early organogenesis

After the mid-hindbrain barrier is established, the hindbrain ventricle forms visibly (blue arrowheads in Figure 4A,G,L; at 10, 10, and 5 dpm in *N. ophidion*, *S. typhle*, and *H. erectus*, respectively) and soon after the first pigment cells can be detected in the dorsal part of the eye's pigment layer and along the trunk (green arrowheads in Figure 4B,G,H,M; at 11 dpm, 10 to 13 dpm, and 6 dpm in *N. ophidion*, *S. typhle*, and *H. erectus*, respectively). Pigmentation continues to spread during the

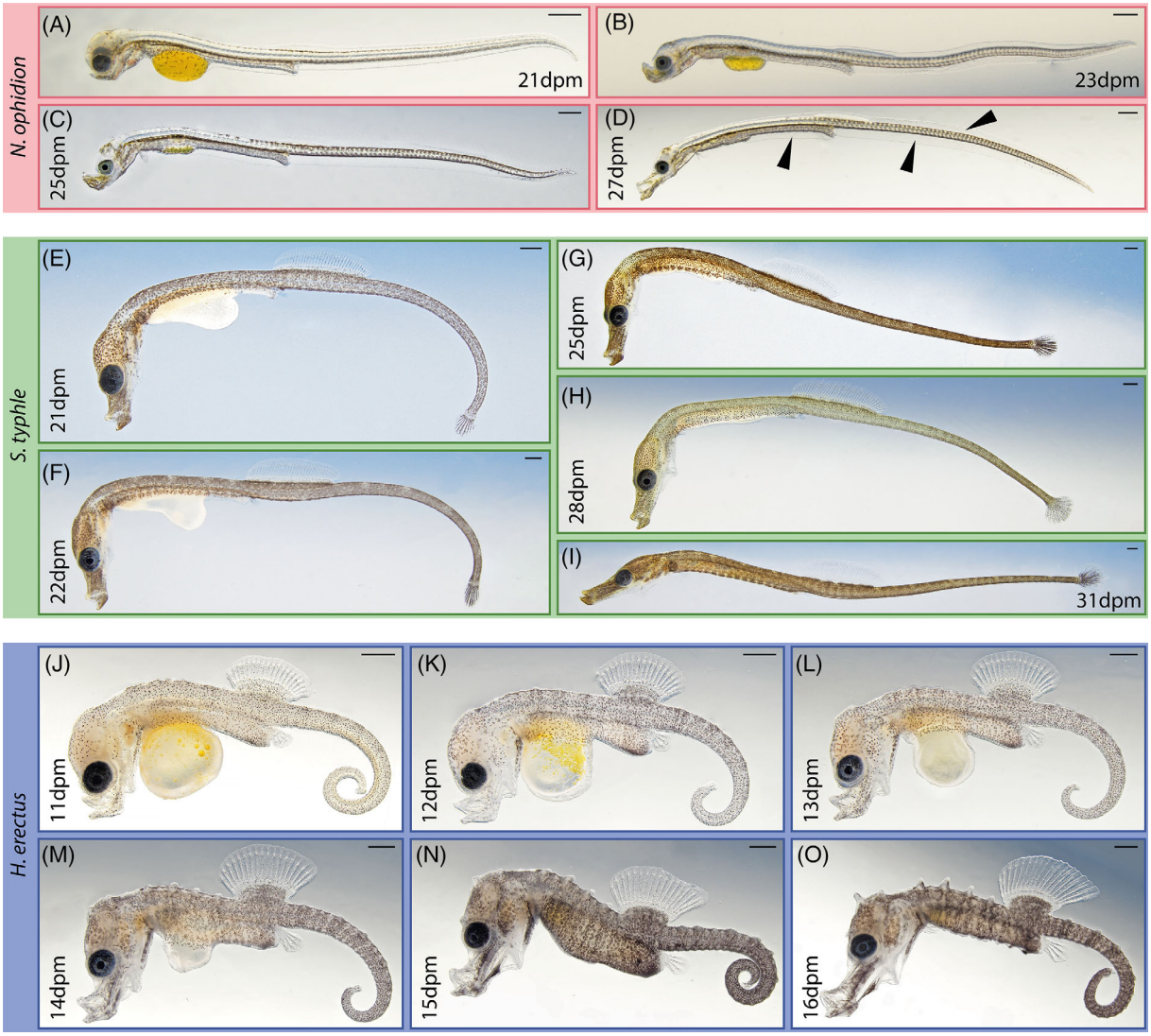

FIGURE 5 Organogenesis to release development in examined syngnathids. *Nerophis ophidion* (A-D), *Syngnathus typhle* (E-I), and *Hippocampus erectus* (J-O), respectively. The last prerelease period is characterized by snout elongation, continued pigmentation and the conclusion of allometric fin outgrowth. Arrowheads: black = fin fold. Scale is 500 μm; dpm = days post mating

following days, especially along the trunk and head, and the eyes become dark and fully pigmented. Somitogenesis continues until 18 dpm in *N. ophidion*, which never develops a caudal fin bud, and until 12 and 7 dpm, in *S. typhle* and *H. erectus*, respectively, after which caudal fin buds form. By 17, 10, and 8 dpm in *N. ophidion*, *S. typhle*, and *H. erectus*, respectively, pronounced mandibular arches have emerged (rufous arrowheads in Figure 4E,I,U in *N. ophidion*, *S. typhle*, and *H. erectus*, respectively), which continuously grow and extend anteriorly. Dorsal fin condensations can be identified after 10 and 6 dpm in *S. typhle* and *H. erectus*, respectively (orange arrowheads in Figure 4G,M in *S. typhle* and *H. erectus*, respectively), while this takes until 17 dpm in *N. ophidion* (orange arrowhead in Figure 4E). The latter species is instead characterized by an outgrowing prominent fin fold along the caudal region, which starts to form at 15 to 17 dpm and is resorbed in the second and third week after hatching (black arrowheads in Figure 4F, 19 dpm). In *H. erectus*, during this period (starting at ~6 dpm; white arrowheads in Figure 4M,N), the hindgut is noticeably increasing in volume, a condition maintained after release.

2.1.4 | Late prerelease development: Organogenesis to release

The last third of prerelease development is characterized by increased pigmentation, yolk sack resorption, the elongation of the tube-shaped mouth, and the appearance of the characteristic bony plates in *S. typhle* and

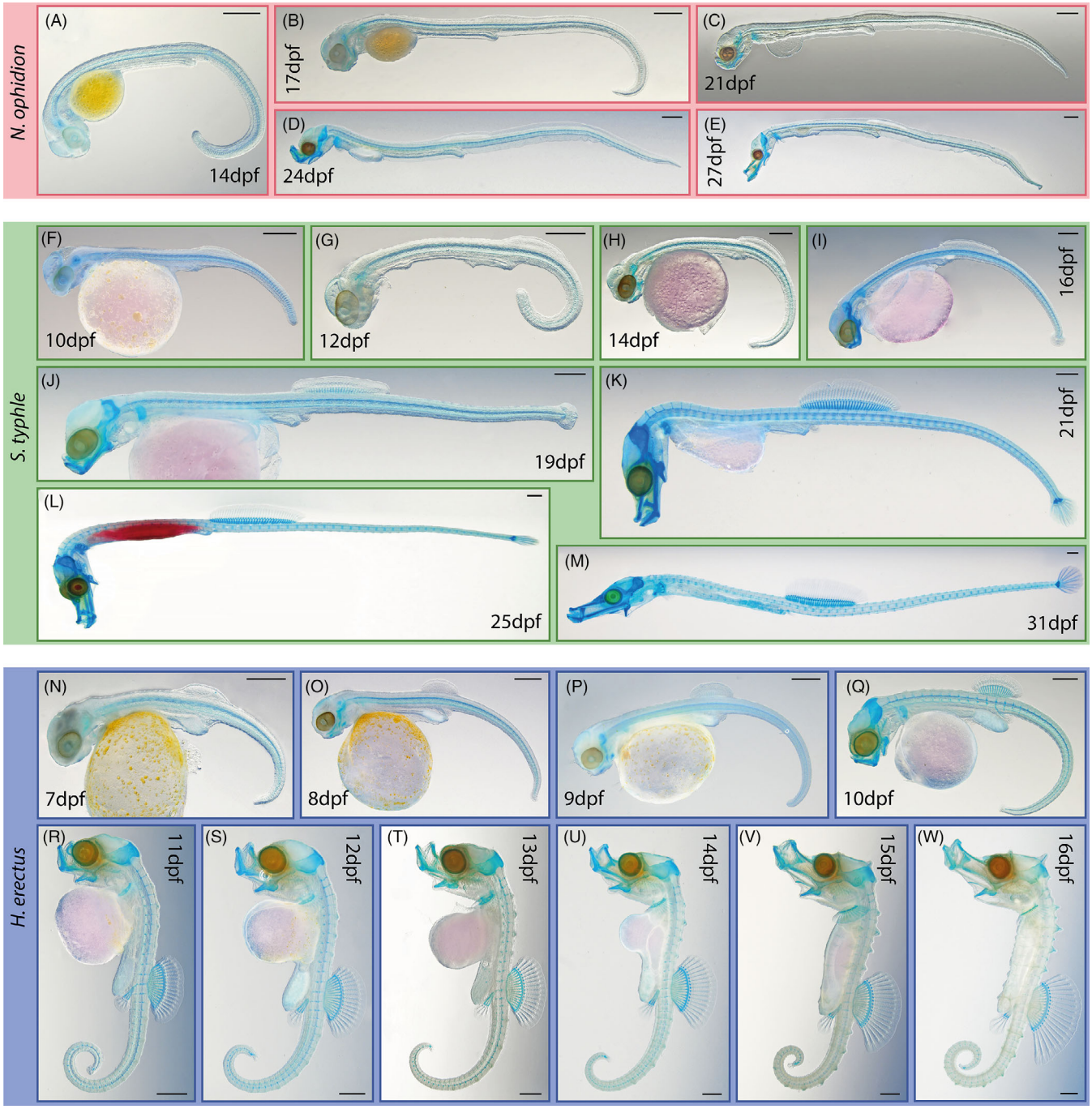

FIGURE 6 Overview of chondrogenesis across investigated syngnathids prenatal development (Alcian blue stained specimens). *Nerophis ophidion* (A-E), *Syngnathus typhle* (F-M), and *Hippocampus erectus* (N-W), respectively. Scale is 500 μm; dpm = days post mating. For red yolk coloration in (L) see Section 5

H. erectus (Figure 5). While *S. typhle* and *H. erectus* become fully pigmented (except for some fins) during this period, *N. ophidion*'s pigmentation is still patchy at the day of hatching and full pigmentation cover of the body is only achieved within the first week post hatching (Figure 5D,I,O in *N. ophidion*, *S. typhle*, and *H. erectus*, respectively; for release day). In all three species, the yolk sack is typically fully absorbed when juveniles are released by their fathers (Figure 5D,I,O in *N. ophidion*, *S. typhle*, and *H. erectus*, respectively). Interestingly, both pipefishes pass through a stage during which their head trunk connection resembles a seahorse. This is most striking in *S. typhle* (which is more closely related to seahorses than it is to *N. ophidion*): from 21 to 28 dpm, the head and trunk are positioned at a right

angle from each other, which becomes only parallel toward release (Figure 5E-I). In contrast in *H. erectus*, the initial right angle between head and trunk never straightens but is maintained in adults, possibly indicative of developmental truncation (Figure 5J-O; see Section 3). At day of hatching, *N. ophidion*'s fin fold is surrounding the caudal and posterior part of the precaudal area (black arrowheads in Figure 5D).

2.2 | Skeletal development as revealed by Alcian blue and Alizarin red staining

The skeletal development of studied species is presented as revealed by Alcian blue (stains cartilaginous tissues blue; Figure 6) and Alizarin red staining (stains ossified tissues red). As delicate ossification appeared undetectable via Alizarin red staining when used as part of the low-acid (and even nonacid) double staining technique in conjunction with Alcian blue in this study,[43] additional Alizarin red staining on selected stages were used to describe ossification patterns separately (see also Section 5). This has also allowed us to detect ossifying tissues earlier than previous studies.[19] A schematic of a *S. typhle* juvenile (chondro)skeleton is used to visualize the position of presented body features in the figures. The branchial basket is not included in the description as the used staining techniques did not reveal its structures sufficiently. Furthermore, individual structures (and substructures) may not be described if they could not be identified with the applied methods. For complementary descriptions of the (cranial) cartilages and bones in syngnathids, see References 9,10,20.

2.2.1 | Chondrocranium: The formation of a tube-shaped snout

One of the most iconic shared features of all syngnathids is their snout-like jaw apparatus, which forms the anterior part of a distinct head (Figures 7-10). The posterior part of the head is connected to the trunk by a neck region that allows for some individualized movement (particularly in the dorsoventral dimension) of the head (depending on the species). The chondrocranium develops throughout the second half and the latter two thirds of prerelease development in the *N. ophidion* and *S. typhle* and *H. erectus*, respectively, and the only structures distinctly stained before were the otoliths/otic cartilage (puce structure in Figures 8A, 9A, and 10A). Using our staining techniques, the earliest non-otic chondric condensations could be identified as the anterior tip of Meckel's cartilage, which scaffolds the dentary (identifiable at approx. 16, 13, and 7 dpm, in *N. ophidion*, *S. typhle*, and *H. erectus*, green structures in Figures 8B, 9A, and 10A, respectively). Most major cranial cartilage condensations could be identified only 1 to 2 days later in all examined species, including the ethmoid plate cartilage, the palatoquadrate, the hyosymplectic cartilage, the ceratohyal and interhyal, and the parachordal cartilage (orange, blue, lime, dark purple, olive, and red structures, respectively, in Figures 8-10). At approximately 20, 17, and 10 dpm, the basihyal, hypohyal, and pterygoid process of the quadrate are recognizable in *N. ophidion*, *S. typhle*, and *H. erectus*, respectively (light violet, English violet, pearly purple structures, respectively, in Figures 8-10D). The mandibular arch becomes more distinct, separates in the maxillary and mandibular process (giving rise to the upper and lower jaw, respectively), and some days later starts to bend upward (dorsally), forming a near vertical orientation of the mouth opening (Figures 8D, 9C, and 10D). At the same time, the upper jaw emerges and while its dorsoventrally aligned jaw position develops after 17 and 10 dpm (corresponding to ~55 and 63% of prenatal developmental time; Figures 9 and 10D) in *S. typhle* and *H. erectus*, this stage of jaw development is reached only after 20 dpm (74% of prenatal developmental time) in *N. ophidion* (Figure 8D). Interestingly, at this stage, the developing ethmoid cartilage is not straight, but rather has a curved shape, which straightens during the last stages of prerelease development (Figures 8-10, orange structures). This is the stage when the iconic snouts forms, starting at about 25 dpm in *N. ophidion* (Figure 8F), 19 dpm in *S. typhle* (Figure 9E) and at about 12 dpm in *H. erectus* (Figure 10E is 13 dpm). Also, during this time the vomer cartilage/rostral cartilage emerges (Figures 8-10, cyan structures), which is accompanied by an overall elongation of the ethmoid and hyosymplectic cartilage in combination with a reorientation of the palatoquatrate, which morphs from its orientation rather parallel to the hyosymplectic cartilage to an orientation almost perpendicular to it. Allometric snout elongation continues after release; however, the composition and relative orientation of morphological structures to each other does not change anymore considerably.

Geometric morphometric data on the head shape and key cartilages was collected and analyzed using principal component analysis (PCA) (see Section 5 for details and limitations of this approach; Figure 11). Note that landmarks used to describe morphological structures were not necessarily truly homologous and thus results have to be interpreted cautiously (see Section 5; Figure 11A). Principal component one (PC1) positively correlates with relative age of the samples, suggesting it reflects the main

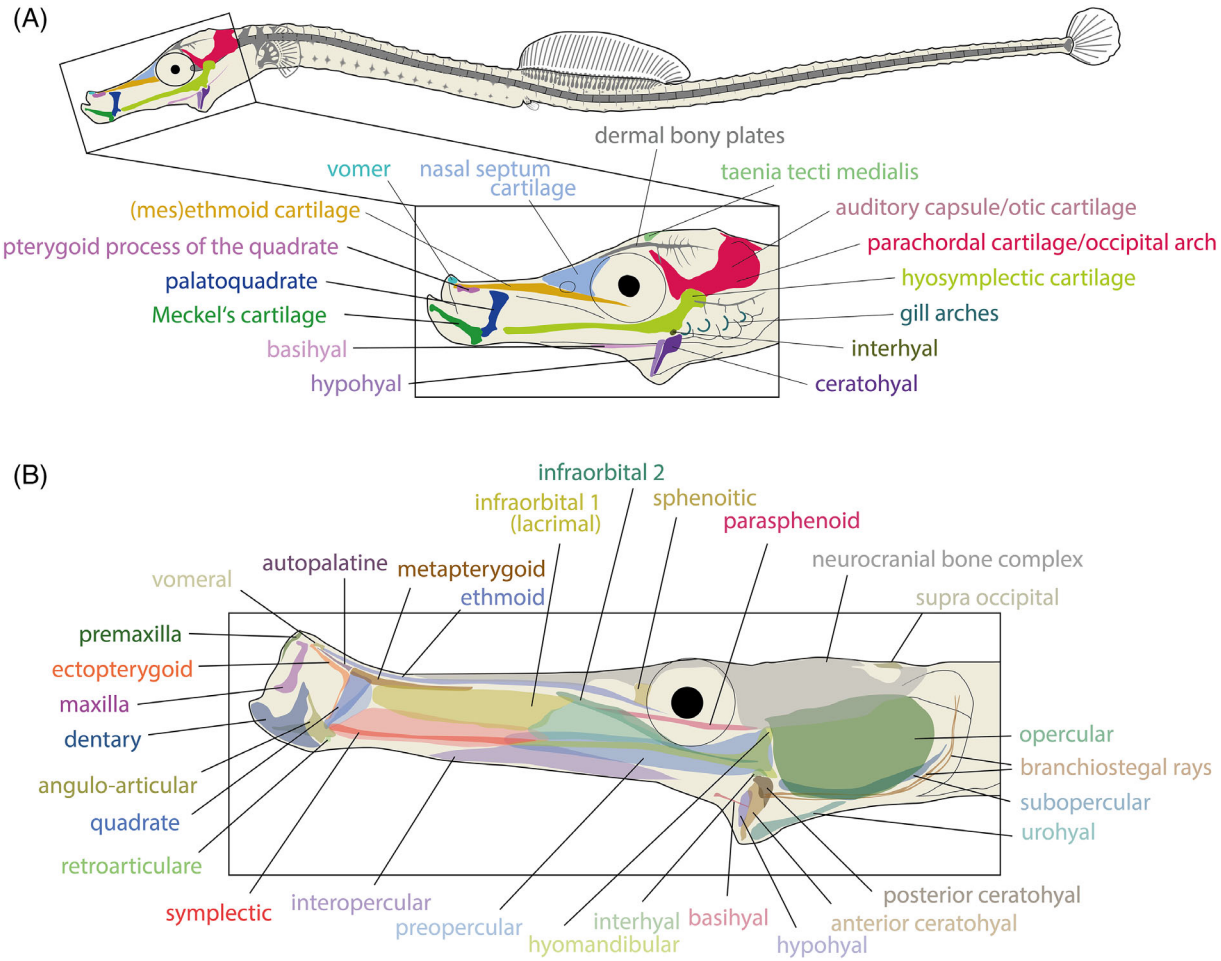

FIGURE 7 Generalized overview of the head skeletons of syngnathids. (A) Head cartilages in syngnathid embryos identifiable after Alcian blue staining in this study. The branchial basket is not detailed. (B) Bones identifiable in adult syngnathids after Alizarin red staining in this study

morphological transitions investigated syngnathids' heads underwent (Figure 11B). At release (rel. age = 1), *S. typhle* individuals show the highest scores (i.e., elongated snout, shallow head) when compared to the other two species, while *N. ophidion* only catches up to *S. typhle* after hatching, and *H. erectus*' scores remain intermediate between the other two species until release. PC2 illustrates how *N. ophidion* undergoes a more pronounced L-shaped jaw stage compared to *S. typhle* (with more negative values on PC2) during its prerelease development (Figure 11C) and only around the day of hatching the snout straightens and a morphology more similar to that of *S. typhle* is developed (i.e., more positive scores on PC2; see also Figure 12A,B). *H. erectus* develops its characteristic high head cranium, which differentiates this species from the pipefish species as reflected on PC3 (Figure 11D).

Using separate Alizarin red stainings, ossification was detected at earlier stages compared to previous studies,[19] and individual bones—especially in the complex head skeleton—could be identified, although individual bones contributing to the neurocranium could not be reliably delineated (Figures 7-10). In all studied species, otoliths were the first structures showing the onset of ossification with this technique (Figures 8-10K, puce arrowheads), followed by the maxillary and cleithrum (purple and orange arrowheads, respectively; 25, 16, and 10 dpm, for *N. ophidion*, Figure 8L, *S. typhle*, Figure 9K, and *H. erectus*, Figure 10L, respectively) and shortly after the premaxillary, symplectic, and dentary (green, red, and blue arrowheads, respectively, Figures 8-10L). In *N. ophidion*, Alizarin red staining suggests that ossification indeed does not commence much further until the larvae hatch and only few more structures show staining, such as the parasphenoid, ceratohyoid, and basioccipital (Figure 8K-M). In *S. typhle* and *H. erectus*, ossification commences much further until the day of release and then can be detected in most facial/cranial bones (Figures 9 and 10K-N; see Figure 7 for annotation).

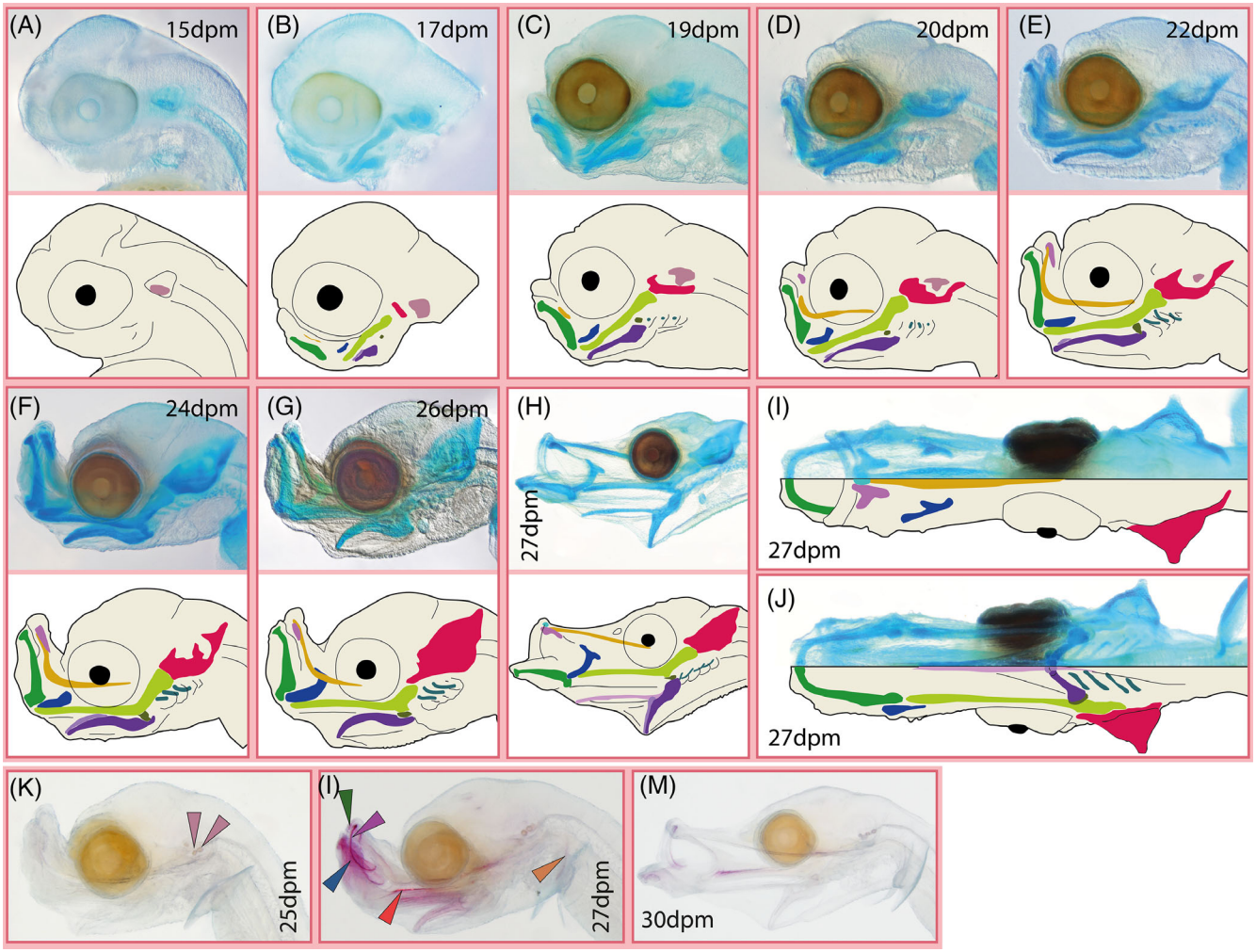

FIGURE 8 Head skeleton of prerelease *Nerophis ophidion*. (A-J) Head cartilages and (K-M) ossifying tissues across the prenatal development; (I) dorsal view, (J) ventral view, all others lateral view. Arrowheads: puce = otoliths, purple = maxilla, red = symplectic, orange = cleithrum, green = premaxilla, blue = dentary; structures of skeletal elements colored according to Figure 7; dpm = days post mating

2.2.2 | Formation of the occipital and precaudal axial skeleton

In vertebrates, the somites contribute to all the body regions except for the anterior head. Four main somite derived skeletal regions are distinguished in fishes, namely the basioccipital (posterior part of head region), precaudal (trunk), caudal (tail), and ural (caudal fin) region.[14] In teleosts, somites 1 and 2 contribute to the basioccipital, which forms the posterior part of the cranium, and somite 3 connects the cranium to somite 4, which represents the first somite developing into a vertebra.[14] We examined the formation of the axial skeleton using Alcian blue and Alizarin red staining. In all three examined syngnathids, the notochord is visible as a subtle blue rod already at very early stages (amber arrowheads, e.g., after 19, 16 , and 8 dpm; Figure 13B,E; H,K; N,Q in *N. ophidion*, *S. typhle*, and *H. erectus*, respectively). The first condensations of the neural arches were observed at the most anterior precaudal somites at 24, 17, and 10 dpm for *N. ophidion*, *S. typhle*, and *H. erectus*, respectively (green arrowheads in Figure 13C; I,L; O,R in *N. ophidion*, *S. typhle*, and *H. erectus*, respectively). It is noteworthy that, whereas in *N. ophidion* 3 days later neural arch formation was still restricted to the most anterior somites (Figure 13D,G), neural arch protrusions were observed in all precaudal and most caudal somites in *S. typhle* and *H. erectus* only 1 day after their first appearance anteriorly (not shown). In *H. erectus* and especially *S. typhle*, the neural arch elements from somites 4 to 6, which correspond to vertebrae 1 to 3, become notably hypertrophic and distinct from other neural arch elements during prerelease development. The first transversal processes were recognizable on central precaudal and anterior caudal vertebrae in *S. typhle* at around

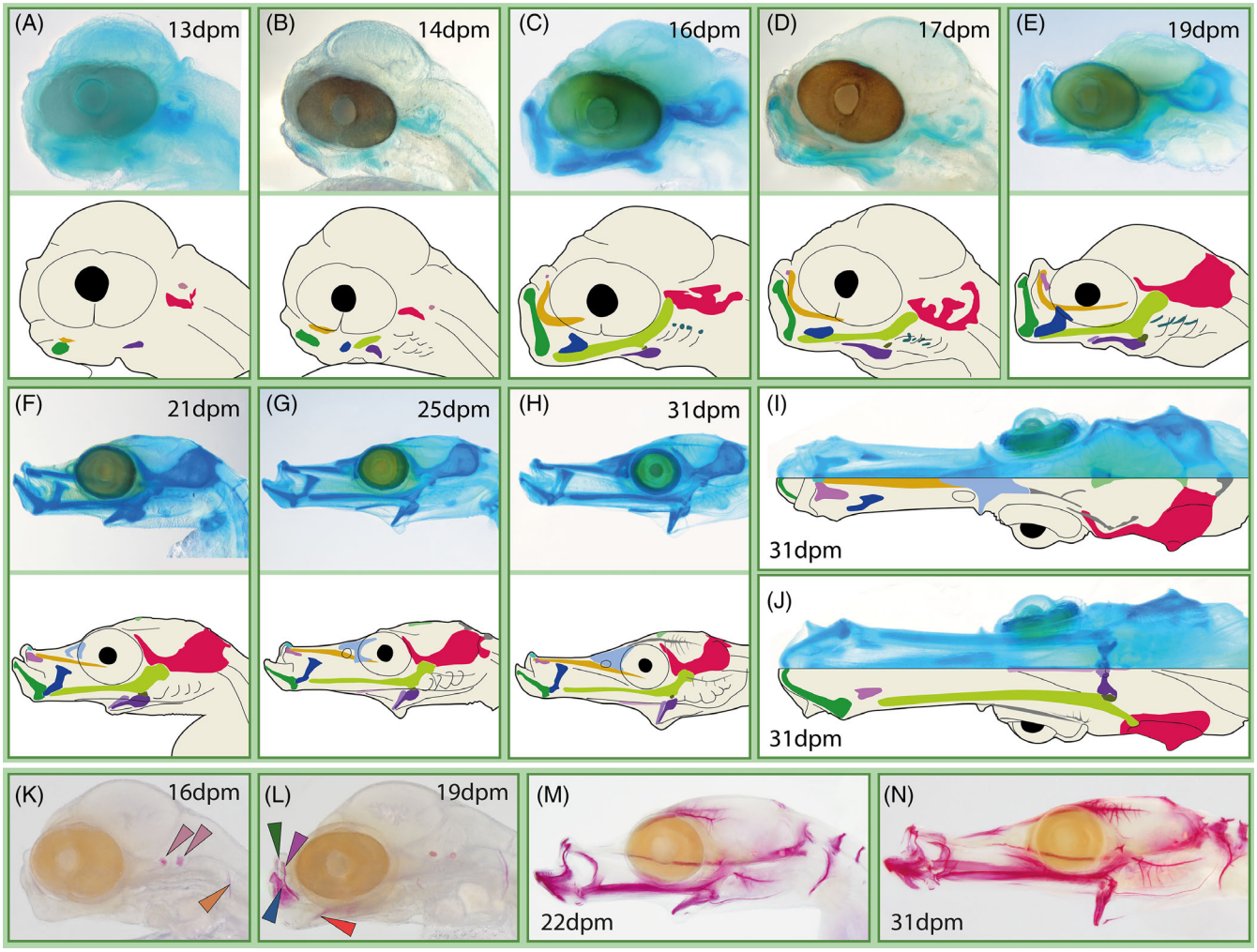

FIGURE 9 Head skeleton of prerelease *Syngnathus typhle*. (A-J) Head cartilages and (K-N) ossifying tissues across the prenatal development; (I) dorsal view, (J) ventral view, all others lateral view. Arrowheads: puce = otoliths, purple = maxilla, red = symplectic, orange = cleithrum, green = premaxilla, blue = dentary; structures of skeletal elements colored according to Figure 7; dpm = days post mating

22 dpm (purple arrowheads in Figure 13I) and in *H. erectus* at 10 dpm (purple arrowheads in Figure 13O,R), while in *N. ophidion* these processes could not unambiguously be identified before hatching day (Figure 13D,G). The formation of the vertebral centra is not detected using Alcian blue because in teleosts, these elements form through intramembranous ossification,[14] and ossifying vertebrae centra are observed via Alizarin red staining at 22 and 16 dpm in *S. typhle* and *H. erectus*, though not in the most anterior vertebrae (see later sections of the manuscript), while no ossification of vertebrae centra could be detected in *N. ophidion* before hatching. In *S. typhle* (Figure 13U) and *H. erectus* (Figure 13W), the neural arches/spines and transversal processes are already substantially ossified at the day of release according to Alizarin red staining (green and purple arrowheads, respectively). Interestingly, Alcian blue stains the non-ossifying part of the vertebral column (as seen in Figure 13I,J), which probably corresponds to the intervertebral disks.

Ribs and epicentrals could not be identified in any of the studied species in line with the notion that syngnathids have secondarily lost ribs,[1] and sesamoid bones in epaxial tendons were only identified in subadult or older stages of *N. ophidion*, but not in *S. typhle* nor *H. erectus*, consistent with previous studies (black arrowhead in Figure 12G).[10,44] The emergence of the hemal arches, which define the caudal region is discussed below together with the developmental of the caudal region.

2.2.3 | Development of the syngnathids' bony plate armor

Adult syngnathids possess an armor of jointed bony plates in their integument,[45,46] which provides protection

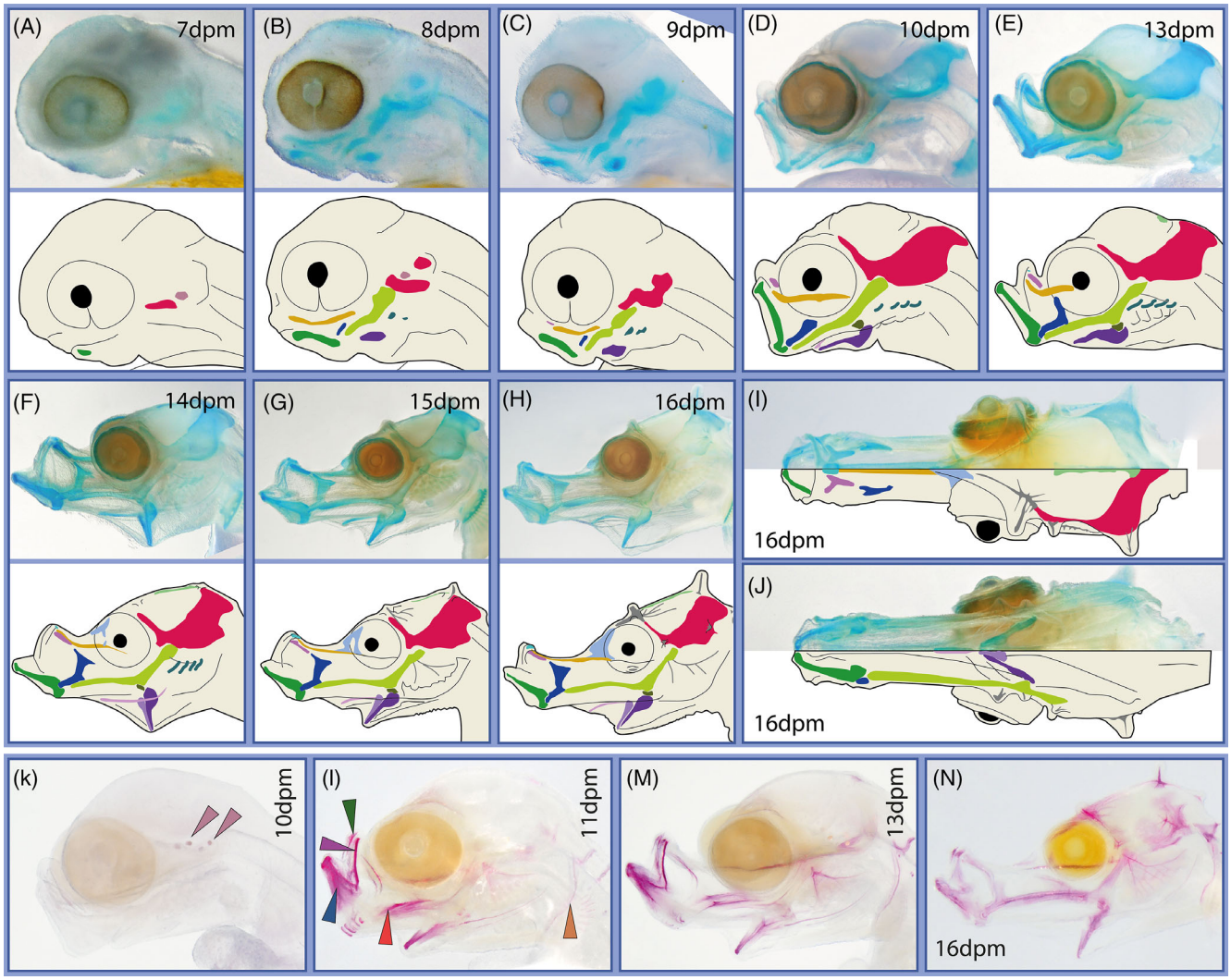

FIGURE 10 Head skeleton of prerelease *Hippocampus erectus*. (A-J) Head cartilages and (K-M) ossifying tissues across the prenatal development; (I) dorsal view, (J) ventral view, all others lateral view. Arrowheads: puce = otoliths, purple = maxilla, red = symplectic, orange = cleithrum, green = premaxilla, blue = dentary; structures of skeletal elements colored according to Figure 7; dpm = days post mating

and structural support for the fins (Figure 1H).[12,47] All three studied species feature a very similar pattern of seven longitudinal (i.e., anterior-posterior) oriented rows of bony plates in the neck and trunk region. Three rows cover each flank in a bilaterally symmetrical pattern whereby the dorsal most rows on each side close in on each other in the dorsal midline (blue row in Figure 14). The ventral side is covered in a single unpaired row of plates (black row in Figure 14), which is discontinued at the anus. In a transition region (approx. from anus to the posterior end of the dorsal fin) the three pairs of flank rows are reduced to the two pairs that form the majority of the square-shaped plate armor of the tail region (with one row forming each edge, Figure 14).[45,47] Interestingly, this transition from six to four rows is different in each species: in *N. ophidion*, the two most dorsal pairs of rows continue seamlessly into the tail region (blue and green rows in Figure 14A); in *S. typhle*, instead, the most dorsal pair of rows is discontinued after the posterior border of the dorsal fin (blue row in Figure 14B) and the remaining two rows form the tail armor (green and orange rows in Figure 14B); and in *H. erectus*, only the middle trunk row is continued as the ventral tail row (green row in Figure 14C), while the dorsal tail row emerges in between the two most dorsal trunk rows at the eleventh plate ring (white row in Figure 14C).

The first putative indications of integument covering in *N. ophidion* occur during the same stages the axial skeleton emerges (Figure 13) and can be observed as one lateral row of pointy spines using Alcian blue (26 dpm;

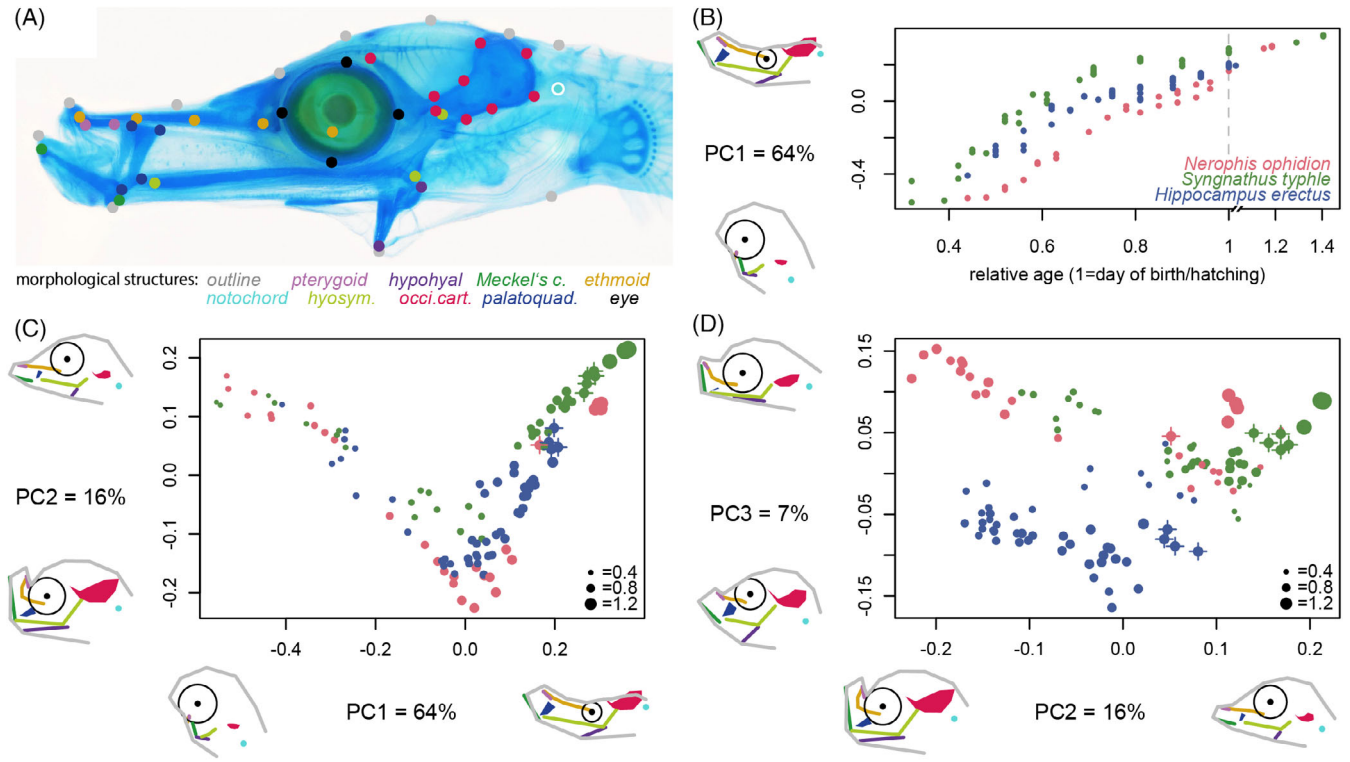

FIGURE 11 Comparative geometric morphometric principal component analysis (PCA) of overall head shape and key cartilages across early development. (A) Forty-four landmarks were used to describe the head shape and key cartilages. In younger specimens, the location of landmarks was estimated as the PCA required a full dataset across all investigated stages. (B) Principal component 1 scores plotted against relative developmental age (i.e., 0 = day of mating, 1 = day of birth/hatching) illustrate dominant morphological variance associated with relative age/size. (C) PC1 and PC2 scores illustrate that all three species undergo a pronounced L-shaped snout stage during development, after which the snout straightens before release. (D) PC2 and PC3 scores illustrate divergent developmental trajectories for the three species. Head shapes illustrate the landmark configurations at the extremes of the respective axis. Dots with crossing lines in (C, D) indicate release/hatching stage and dot size reflects relative age. Structures of skeletal elements colored according to Figure 7

compare to white arrowheads in Figure 13D,G; which here probably is indicative of dermally ossifying condensations with high glycosaminoglycan content, rather than of cartilage). Together with spines formed by cranial cartilages (see Figure 7I,J) *N. ophidion* larvae exhibit thus a row of defensive spines along the body, which is only resorbed 1 to 2 weeks after hatching and likely functionally replaced by the adult bony plate armor. It remains unclear if these spines are developmental precursors of bony plates or have an independent origin. Notably, similar protrusions are also observed in *H. erectus*, starting at ~12 dpm (blue arrowheads in Figure 13O,R,P,S). Here, protrusions remain blunt and become bony plate centers. Given the apparently divergent ontogenetic trajectories the homology between the early dermal protrusions in *N. ophidion* and *H. erectus* remains (and to a lesser degree *S. typhle*, Figure 13J,M) for now unclear.

Adult *N. ophidion* and *S. typhle* have similar plate types and individual plates are connected by well-developed longitudinal spine-and-groove joints and smaller (or absent) transversal peg-and-groove joints (Figure 15A-C; for details on plate ultrastructure see Reference 46). Their bony plates develop from cross-shaped tissue condensations ("ridges") that stained blue with Alcian Blue (observable from 10 days post release and 28 dpm onward in *N. ophidion* and *S. typhle*, respectively, see Figure 13J,M for *S. typhle*). These crosses emerge along the body in aforementioned rows, with one cross being formed per vertebra and row. Crosses then continue to form the main ossification ridge of maturing bony plates throughout further development as they expand, ossify and get into contact with each other (Figure 15D). When forming bony plates start to overlap peg-and-groove sliding joints are formed with the more cranially oriented margin of a plate always sliding over its neighboring plate and, by doing so, forming the groove. The more caudally oriented margin slides under its neighbor and forms the peg (white arrowheads in Figure 15A-D). In addition, a plate's dorsal margin slides over its more dorsally situated neighbor, and one or

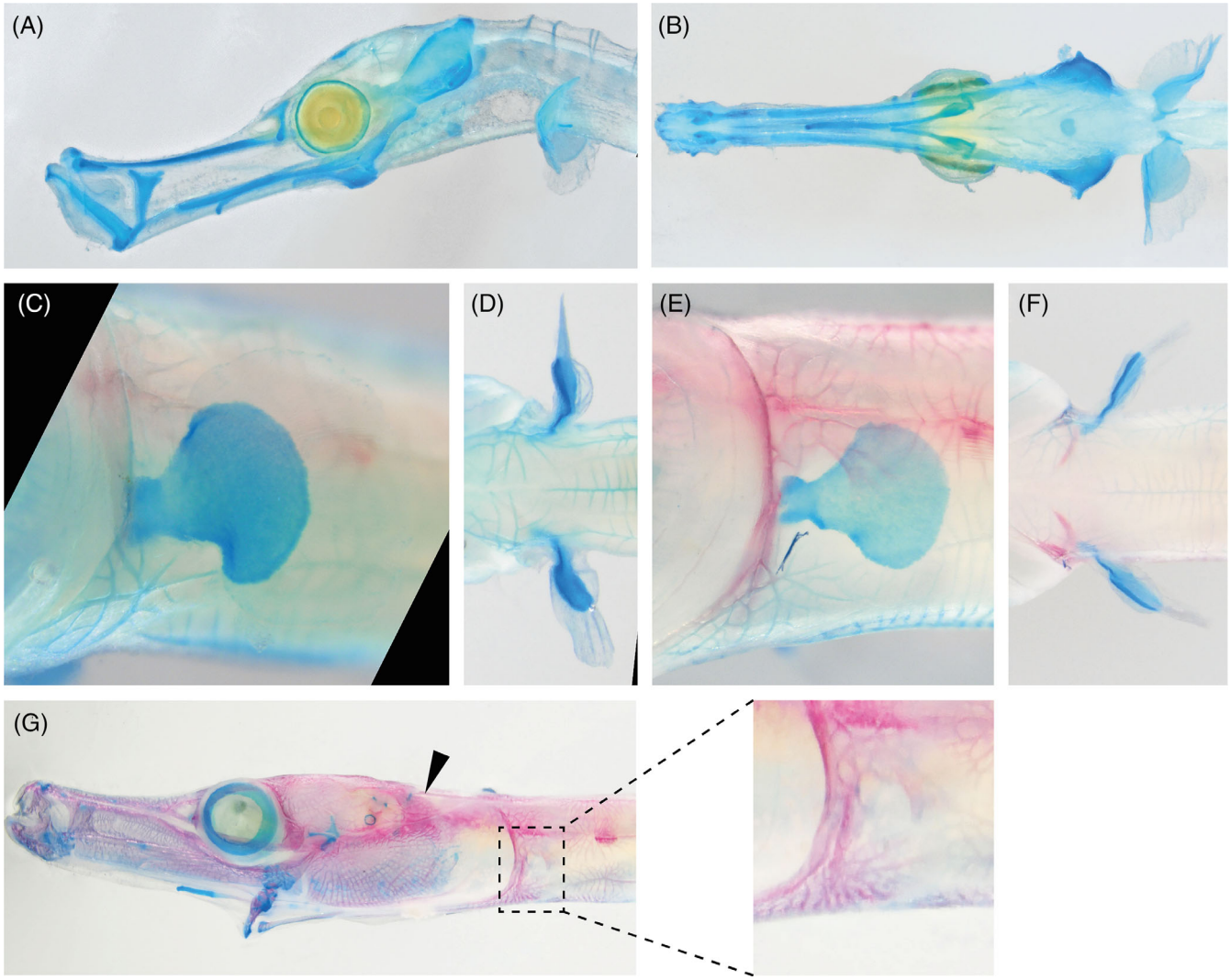

FIGURE 12 *Nerophis ophidion* cranial and pectoral development post hatch. A, C, E, G = lateral views; B, D, F = ventral view; A, B = 10 days post hatch, C-G = later subadult stages, wild-caught individuals. Black arrowhead = epaxial sesamoid bone in *N. ophidion*

multiple joints may be formed (black arrowheads in Figure 15A-D). In *H. erectus*, plates are connected by exactly one well developed peg-and-groove joint to each adjacent plate (dorsoventral joints indicated by black arrowheads in Figure 12E-H). In studied pipefish, only longitudinally oriented joints (i.e., joints to cranially or caudally adjacent plates; white arrowheads in Figure 15A-D) form such well-developed joints, while those between dorsoventrally overlapping plates remain often much less well developed (black arrowheads in Figure 15B,C): here, several smaller joints can be found (especially in the precaudal region) or joints can be absent (especially in the caudal region), suggesting different evolutionary demands for skeletal flexibility among species and body regions within species.[45,47] Furthermore, the shape of these plates in studied pipefishes could be visualized using Alzarin red staining only relatively late in development (for both pipefish species, weeks after hatching/birth), suggesting that rigidity of the bony plate armor remains low until late in development, while in *H. erectus*, this was already possible few days post birth, arguing for a high rigidity of the seahorse's body armor in early stages compared to those of studied pipefishes. Still, in *S. typhle*, we observed that some of the spaces between these bony plates become filled by much smaller, secondary plates without joints in adults, which do not arise from (or feature) previously described ridges (see also Reference 46), arguing for the importance of a body armor that covers the body fully.

Finally, in *H. erectus*, the cross-shaped condensations that form the bony plates are often elevated upon spine-like protrusions (primarily on the most dorsal plate row; not to be confused with spine-like protrusions found in *N. ophidion*), visible from ~12 dpm onward (blue

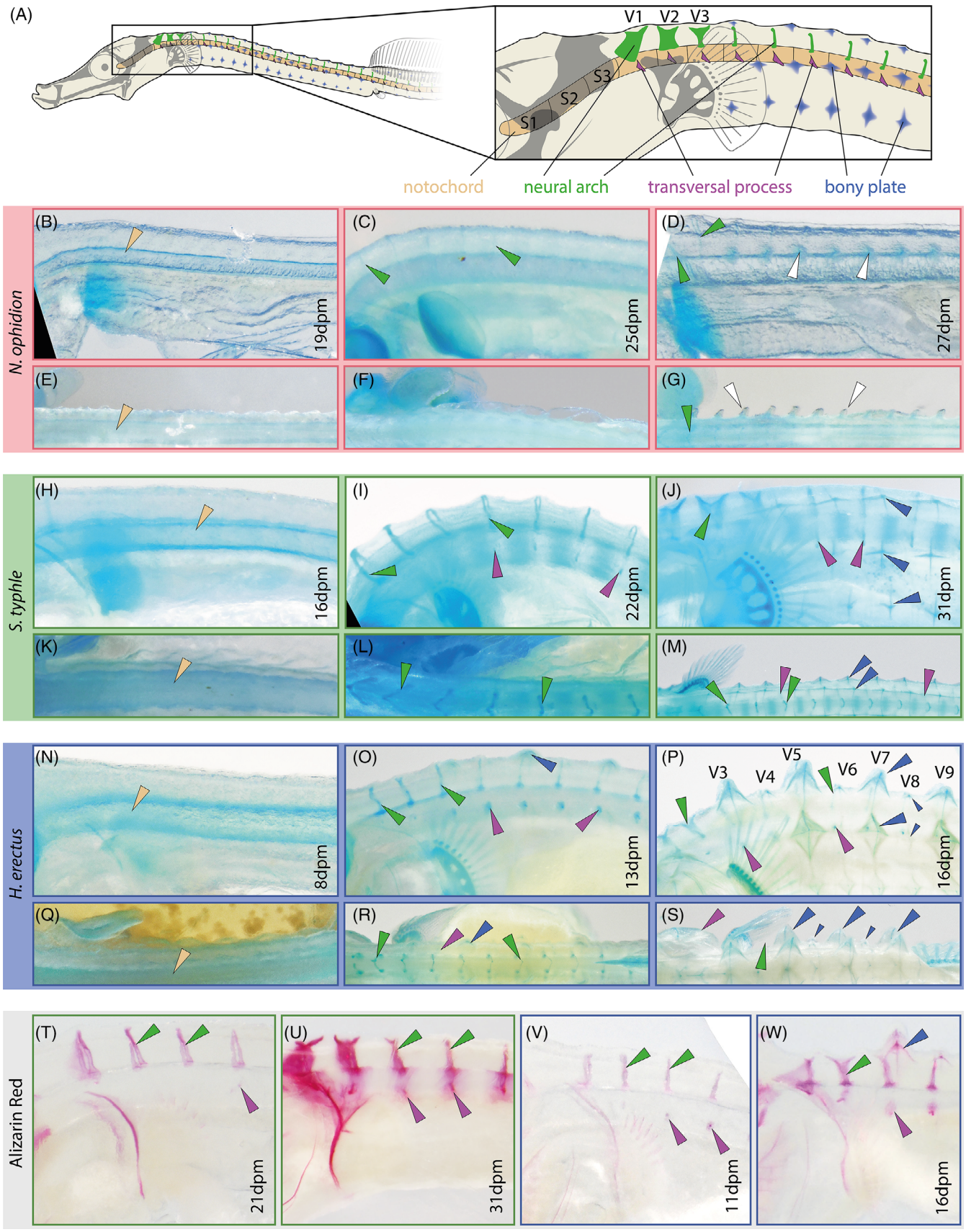

FIGURE 13 Legend on next page.

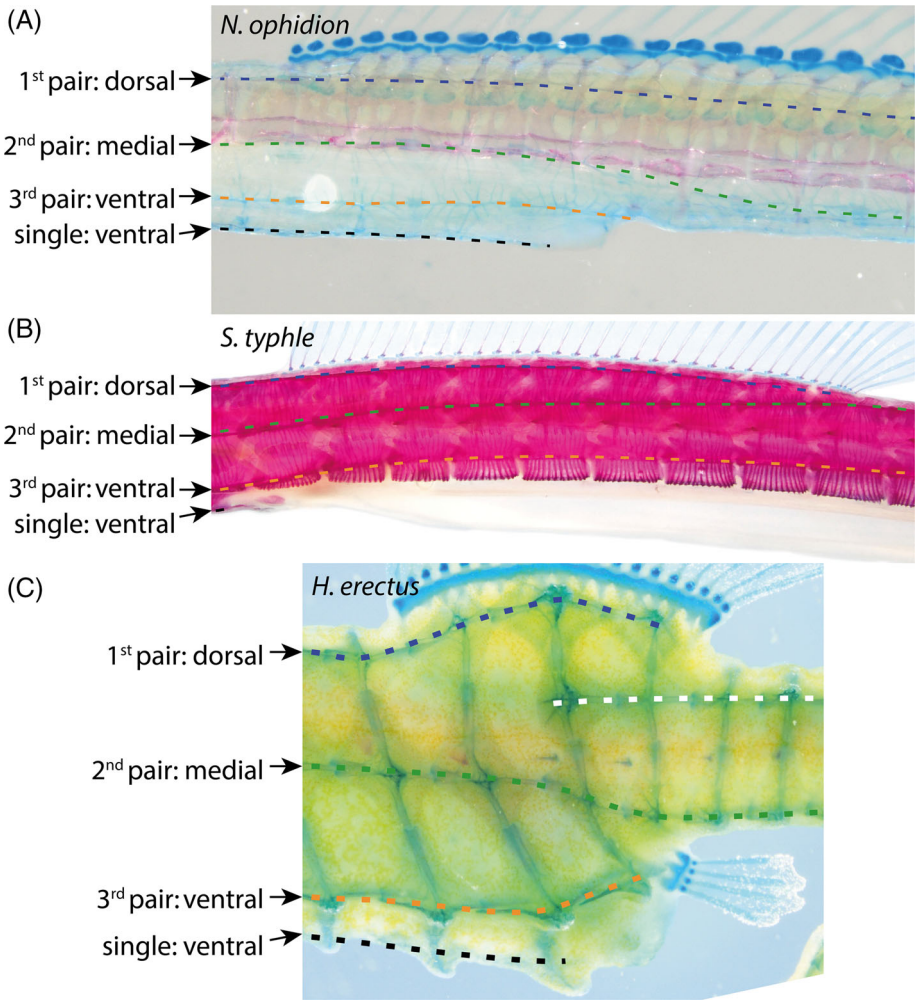

FIGURE 14 Bony plate transition from precaudal to caudal. The transition of the seven rows of bony plates on the precaudal region *n* into four rows on in the caudal region differs among species. (A) *Nerophis ophidion*, (b) *Syngnathus typhle*, and (c) *Hippocampus erectus* from a lateral view (cranially left, dorsal up); individuals stained with Alcian blue and/or Alizarin red

arrowheads in Figure 13P,S). Interestingly, these plate protrusions emerged consistently among individuals first on the precaudal vertebrae three, five, seven, and nine, while protrusions on the other precaudal vertebrae only emerged much later and remain smaller (hypertrophic vs hypotrophic plate protrusions, respectively). Caudally to the dorsal fin, such hypertrophic protrusions are found every three to four vertebrae, with individuals varying in patterns: some have hypertrophic protrusions consistently on every third caudal vertebra, some on every fourth, and others have more variable patterns. The difference between hypertrophic and regular spine-like protrusions translates also in differences in bony plate sizes, which are most notable in juveniles in *H. erectus*, while in adults the differences are much less pronounced (but still recognizable).

2.2.4 | Pectoral fin and girdle morphology: Loss and degeneration

The characterization of the morphology and developmental history of the syngnathids' pectoral girdle and fin has been challenging due to their high degree of ossification as well as bone fusions and resorptions in juveniles and adults. Furthermore, the unusual positioning and shape of the endochondral disk derived bones in these fish led to some incorrect conclusions in previous studies (Figure 16).[17] The adult pectoral fins of *S. typhle* and *H. erectus* are highly derived and characterized by fusion with the bony plate armor and resorption of central fin parts. In *N. ophidion*'s rudimentary pectoral fins are only present in embryos and larvae, but are resorbed upon transition into juveniles (Figure 12C-G).

FIGURE 13 Development of the syngnathids' axial skeleton. (A) Main skeletal structures contributing to the anterior axial skeleton in juvenile *Syngnathus typhle*. (B-S) Cartilaginous structures stained by Alcian blue and (T-W) mineralized structures stained by Alizarin red in examined syngnathids. (B-D, H-J, N-P, T-W) Lateral view, (E-G, K-M, Q-S) dorsal view. (A-G) *Nerophis ophidion*, (H-M, T, U) *S. typhle*, (N-S, V, W) *Hippocampus erectus*. Arrowheads: amber = notochord, green = neural arch/spines, blue = bony plate protrusions, purple = transversal process; dpm = days post mating

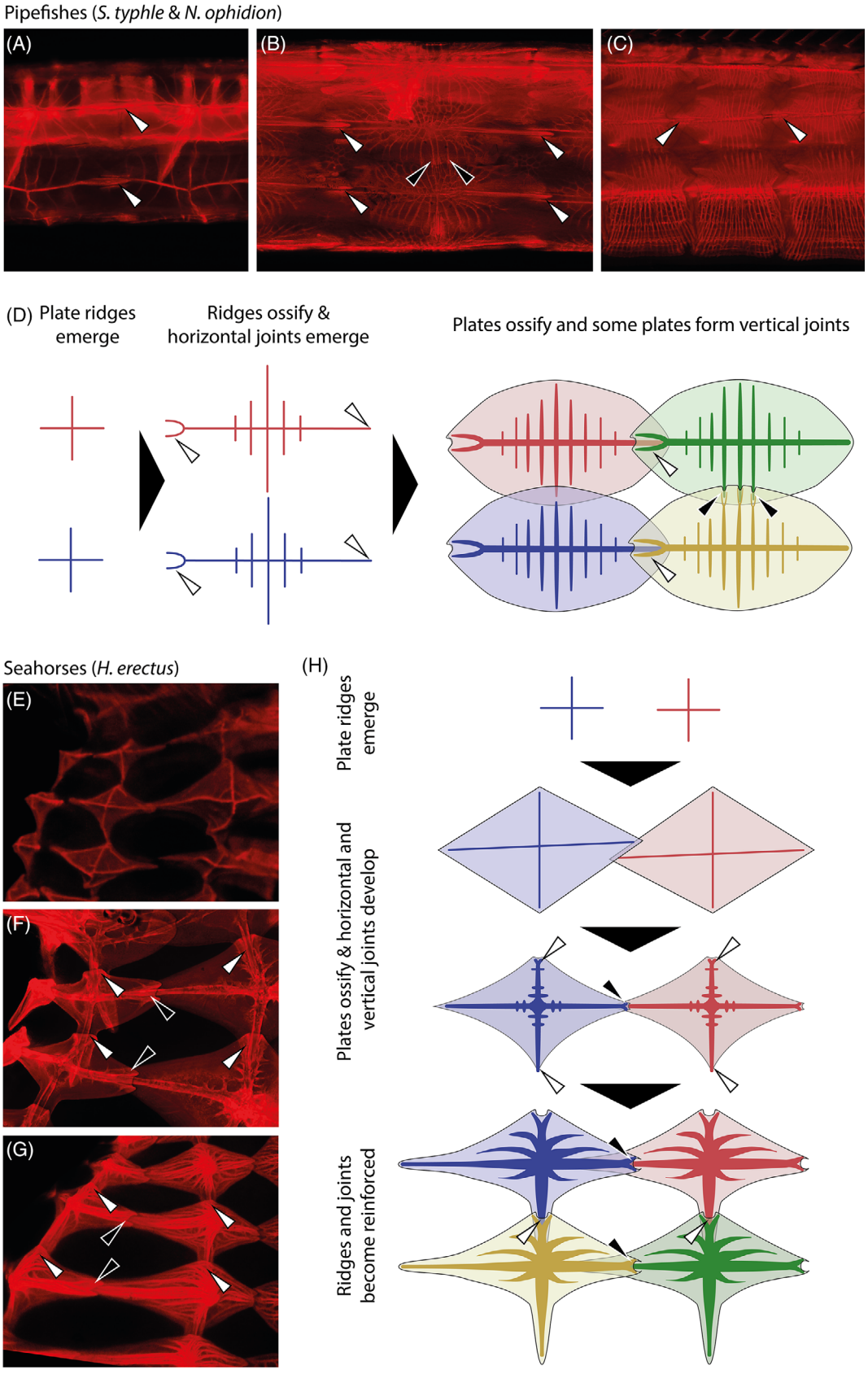

FIGURE 15 Legend on next page.

In all three species, pectoral fin bud condensation could be observed early on in development (Figure 2) and an endoskeletal disk (giving rise to the scapula, coracoid, proximal radials [blue gray structures in Figure 16A,B,F,G] and a presumed propterygium [purple structure in Figure 16A,B,F,G]) could be recognized via Alcian blue staining from 14, 15, and 6 dpm in *N. ophidion*, *S. typhle*, and *H. erectus*, respectively (blue gray and purple arrowheads in Figure 17A,E,M). Shortly after the pectoral fin bud emerges, the cleithrum starts to form in all three species (orange arrowheads in Figure 17B,F,N). A main difference to most other teleosts is the failure of the endoskeletal disk cartilage to separate the initial cartilaginous Anlage into discrete scapula, coracoid and proximal radial elements during prerelease development. In *S. typhle* and *H. erectus*, a continuous Anlage emerges oriented almost perpendicularly to the body axis (blue gray arrowheads in Figure 17l,T). Along its proximal ridge, a forked thickening corresponds to a scapulocoracoid, which initially remains distally fused to the distal part of the endochondral disk (blue gray structures in Figure 16B; blue gray arrowheads in Figure 17l,T). In other teleosts, this more distal part of the endochondral disk gives rise to the proximal radials through cartilage resorption (dark blue gray structures in Figure 16B); however, in syngnathids, this process appears to be partially suppressed. In *S. typhle* and *H. erectus*, initial central fissures form, but these fail to extend proximally and distally before release (Figure 16B; Figure 17l,T). The recognizable five radial elements (the most dorsal one probably corresponding to the propterygium; purple structure in Figure 16A,B) remain fused distally and proximally connected to the scapulocoracoid—a conformation retained until bony plates covering the pectoral girdle have ossified sufficiently weeks to months after release (Figure 16D-K).

Distal radials and fin rays appear as de novo condensations approximately 20 and 10 dpm in *S. typhle* and *H. erectus*, respectively, and resemble in their ontogeny and structure those of other teleost fins (rose and green arrowheads indicate distal radials and fin rays, respectively, in Figure 17I,Q for *S. typhle* and *H. erectus*, respectively).[9] In adult *S. typhle* and *H. erectus*, the pectoral fin complex is attached to, and largely obscured by, strongly ossified tissue (Figure 16D) and its morphology is therefore difficult to observe. Dissections reveal the presence of seemingly five proximal radial elements, which have now become attached to the dermal armor (dark blue gray arrowheads/structures indicate proximal radials in Figure 16D-G). At their distal end, proximal radials (dark blue gray structures/arrowheads in Figure 16A-J) remain connected to each other via cartilaginous tissues and articulate with the fin rays (lepidotrichia) through the distal radials (green and rose structures, respectively, in Figure 16A,B). Only a ventroproximal rudiment remains of the scapulocoracoid (light blue gray structures/arrowheads in Figure 16H-K) and proximal radials are individualized proximally. The radial elements do thus not directly articulate with the girdle but are fixed in place by their attachment to the bony armor; however, the two are connected through the dorsoventral fin musculature that bridges the large intervening gap (violet structures in Figure 16F,G). The bony plates associated with the rudimentary girdle and radials probably provide the structural support that allowed the evolutionary reduction of radial and girdle elements. Thus, in adult *S. typhle* and *H*. erectus, the pectoral fin/girdle is a highly derived complex wherein five radial-like elements are attached to the bony armor posterior-distally and the girdle is present as a small scapulacoracoid element anterior-proximally attached to the cleithrum and dermal plates (light blue gray and orange structures/arrowheads, respectively, in Figure 16A-J). Interestingly, the presence of five, instead of four, radials might equally be interpreted as a derived departure from the canonical Bauplan of the teleost fin.[48] We, however, speculate that the most dorsal (rudimentary) radial element corresponds to the propterygium, whose formation and subsequent secondary fusion with the coracoid can also be observed in cichlids (purple structures/arrowheads in Figure 16).[14]

Altogether, and while the homology of the various elements of the pectoral fin cannot yet be resolved with complete certainty, it appears that the autoapomorphic pectoral fin of *H. erectus* and *S. typhle* results from a failure to separate the initial endochondral disk into the separate components of the ancestral teleost pectoral fin, followed by a resorption of most of the initial cartilaginous *Anlage*.

An even more extreme developmental modification is found in *N. ophidion*, where pectoral fin development is truncated at the endochondral disk stage. During embryogenesis, a single continuous endochondral disk

FIGURE 15 Postnatal development of the syngnathids' bony plates. (A-C, E-G) Alizarin red fluorescence (stains ossified tissue) visualizes the development of bony plates, lateral view. Juvenile (A) and adult (B) *Nerophis ophidion* (here: trunk region) and (C) adult *Syngnathus typhle* (here: caudal region; all cranial leftward and ventral downward. *Hippocampus erectus* neck regions of an individual few days post birth (E), few weeks post birth (F) and adult (g; cranial to the top, ventral leftward). Arrowheads: white = longitudinal spine-and-groove joints, black = transversal joints

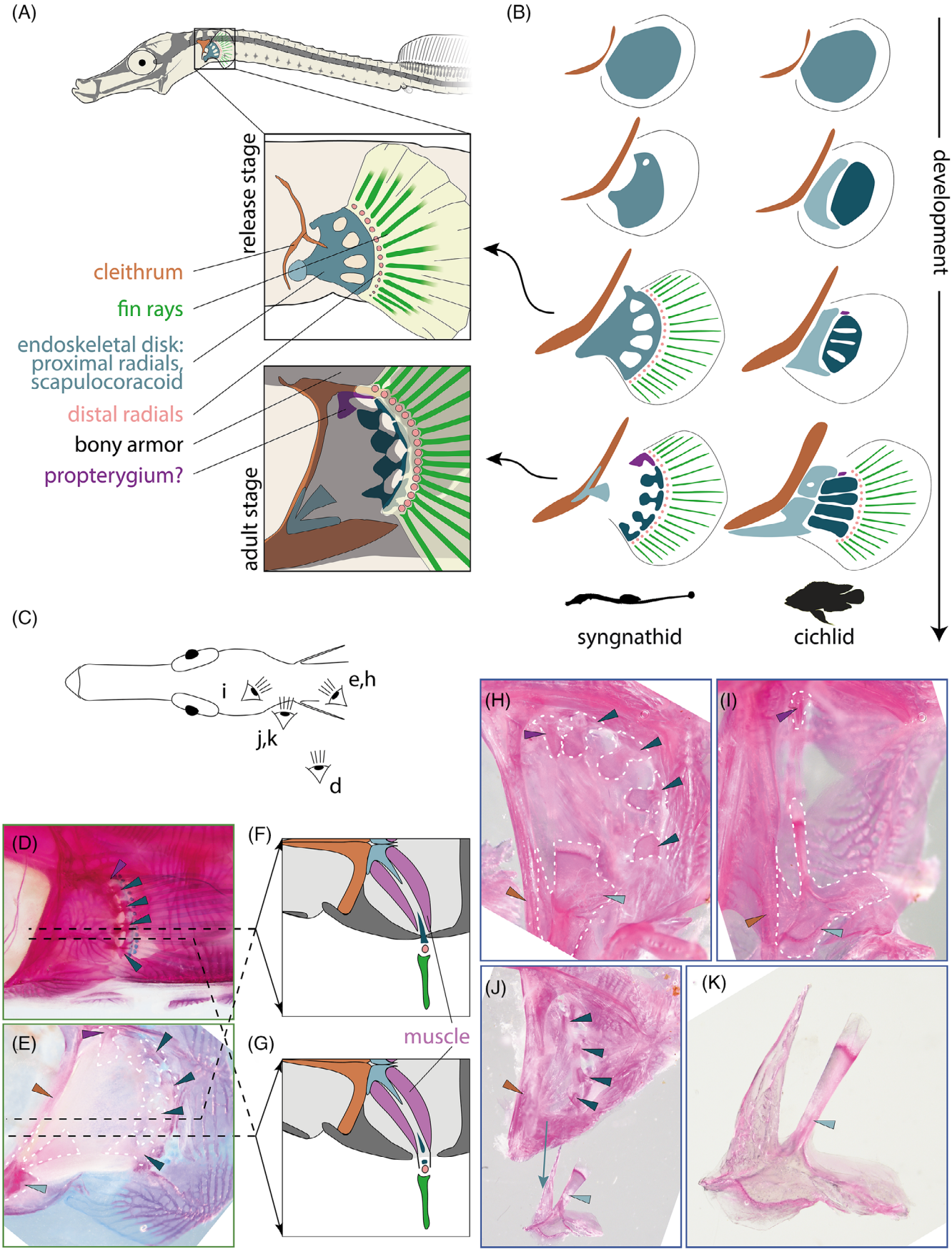

FIGURE 16 Legend on next page.

Anlage connected to a fin fold is formed (blue arrowheads in Figure 17A-D). However, this disk never shows any fissures nor do distal radials or fin rays develop. Instead, pectoral fin differentiation is terminated after approximately 21 dpm (after which only the fin fold is still allometrically growing; Figure 17C). Larval *N. ophidion* use these neotenic pectoral fins throughout their first post-release life stages (approx. the first 2 weeks post hatch), but lose them finally while transitioning into juveniles, which only possesses a dorsal fin after loss of the neotenic pectoral fins (Figure 12C-G).

2.2.5 | Development of the caudal axial skeleton, dorsal fins, and anal fins

The transition from precaudal to caudal vertebrae is indicated by the presence of the hemal arch in caudal vertebrae (red arrowheads in Figure 18A), which forms from protrusions found at 18 and 9.5 dpm in *S. typhle* and *H. erectus*, respectively (Figure 18J,R, respectively), while these are not present yet in *N. ophidion* at hatching (Figure 18E; at 10 days post hatch, they could be observed using Alcian blue staining). Commencement of vertebrae centra ossification could be first detected the transition zone from precaudal to caudal at 21 and 15 dpm in *S. typhle* and *H. erectus*, respectively (not shown, but see Figure 18V,Y). The dorsal fin develops from mesenchymal condensations, which first form the proximal radials (pterygiophores; observable after 27, 17, and 8 dpm; in *N. ophidion*, *S. typhle*, and *H. erectus*; Figure 18E,I,P, respectively; light blue arrowheads). In *S. typhle*, the distal radials and finally rays follow (rose and green arrowheads, respectively, in Figure 18J, 18 dpm) while in *H. erectus*, rays appear before distal radials (green and rose arrowheads, respectively, 9.5 and 10 dpm, Figure 18R,S, respectively). In *N. ophidion*, dorsal fin differentiation is not concluded before hatching, likely because the species relies on its well-developed fin fold for locomotion during the first days post hatching (black arrowheads in Figure 19D-F), but at approximately 12 days post hatch rays were completely formed (data not shown). Seahorses rely for their locomotion on dorsal fin movement.[49] In line with this central importance seahorses complete dorsal fin formation relatively earlier in development, even compared to *S. typhle*. In *S. typhle* and *H. erectus*, the anal fin forms in a similar sequence to the dorsal fin, but development is slower and delayed in *S. typhle* (Figures 2 and 18K-M), while it is more synchronized with the dorsal fin in *H. erectus* (Figures 2 and 18S-U). For the dorsal fins, Alizarin red staining indicated mineralization commences simultaneously in the fin rays and proximal radials (green and light blue arrow heads, respectively, in Figure 18V,X in *S. typhle* and *H. erectus*, respectively). While the anal fin ossified synchronized with the dorsal fin in *H. erectus* (Figure 18X,Y), no ossification could be detected in this fin in *S. typhle* prerelease.

2.2.6 | Ural region and the caudal fin

The teleosts' caudal fin is a complex structure and, in contrast to the other fins, its endochondral components are derived from the vertebral column. In the caudal fin, rays articulate directly with highly modified neural and hemal arches (the "epurals" and "hypurals," respectively), which originate from the most posterior vertebrae (for overview, see Reference 14). In syngnathids, the caudal fin was lost in several taxa (often in favor of a [semi-] prehensile tail),[45] and in those with caudal fins it appears highly derived (Figure 19A). From among the many individual bony structures found in most other teleosts, only the urostyle (or a urostyle-like most posterior element) could be identified with some certainty in *S. typhle* and *H. erectus* (ochre arrowheads in Figure 19H-J, R, S, ii), although in the latter it does not retain its initial dorsal bending (visible at 8 dpm; ochre arrowhead in Figure 19S), which would be typical for teleost fishes. In *S. typhle*, the formation of a single hypural cartilage can be observed (18 dpm; blue arrowhead in Figure 19N). Its partially bifurcated shape is suggestive of specification into a dorsal and a ventral domain. This cartilage does however not separate into individual hypural radials. In this species, actinotrichia can already be observed at 17 dpm (green arrowhead in Figure 19M) and forming fin rays directly articulate with the hypural cartilage

FIGURE 16 Pectoral fin base skeleton in syngnathids. (A) Main skeletal structures contributing to pectoral girdle and fin in juvenile *Syngnathus typhle*. (B) Comparison of main pectoral fin skeletal elements across developmental stages and between species; cichlid development following.[14] (C) Viewing angles of plots (D) (left pectoral fin) and (E, H-K) (right pectoral fin/girdle) after dissection. (D, E, H-K) Alizarin red and Alcian blue stains of adult *S. typhle* (D, E) or *Hippocampus erectus* (H-K). (F, G) Schematic dorsal view on the bone architecture of the pectoral fin at two different positions on the pectoral girdle (lateral downward, medial upward). Soft tissue attached to the scapulocoracoid and radials not removed (E) or removed (H-K). (H-K) Detailed view on the scapulocoracoid's position and its morphology. Arrowheads: purple = alleged propterygium, dark blue gray = proximal radials, light blue gray = scapulocoracoid, orange = cleithrum

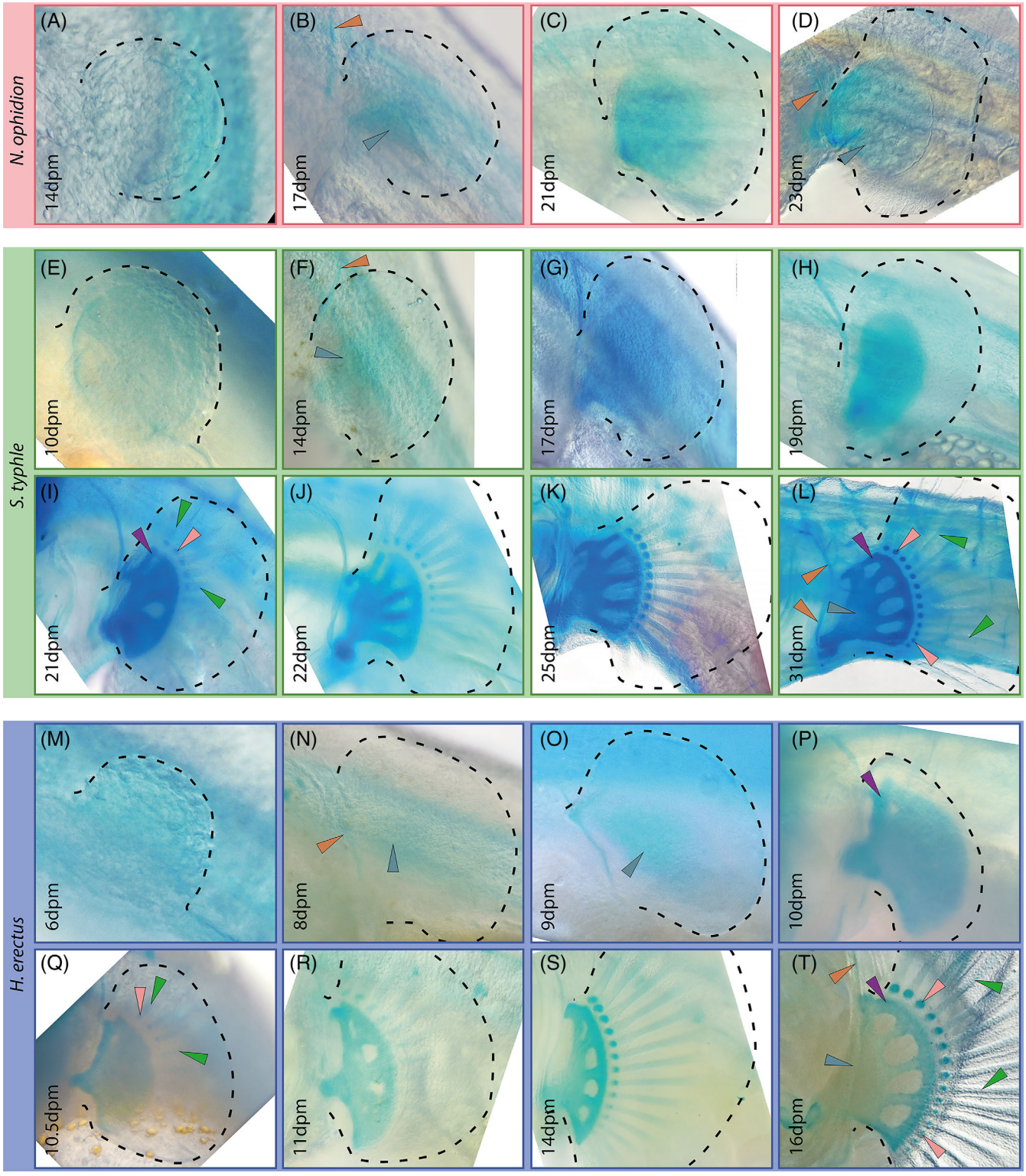

FIGURE 17 Pectoral fin chondrogenic development in examined syngnathids. Pectoral fin development as revealed by Alcian blue staining. (A-D) *Nerophis ophidion*, (E-L) *Syngnathus typhle*, and (M-T) *Hippocampus erectus*. All lateral view but (H) is transversal view after surgical removal of trunk. Arrowheads: orange = cleithrum, green = fin rays, purple = alleged propterygium, blue gray = endoskeletal disk, rose = proximal radials; dpm = days post mating

(starting approx. 19 dpm; Figure 19N-P). This morphology is still present in adult *S. typhle*; however, it should be noted that bony plates cover the entire tail up to the caudal peduncle, presumably providing structural stability to the caudal complex (similar to the pectoral fins). In *S. typhle*, the presence of an additional transient dorsal

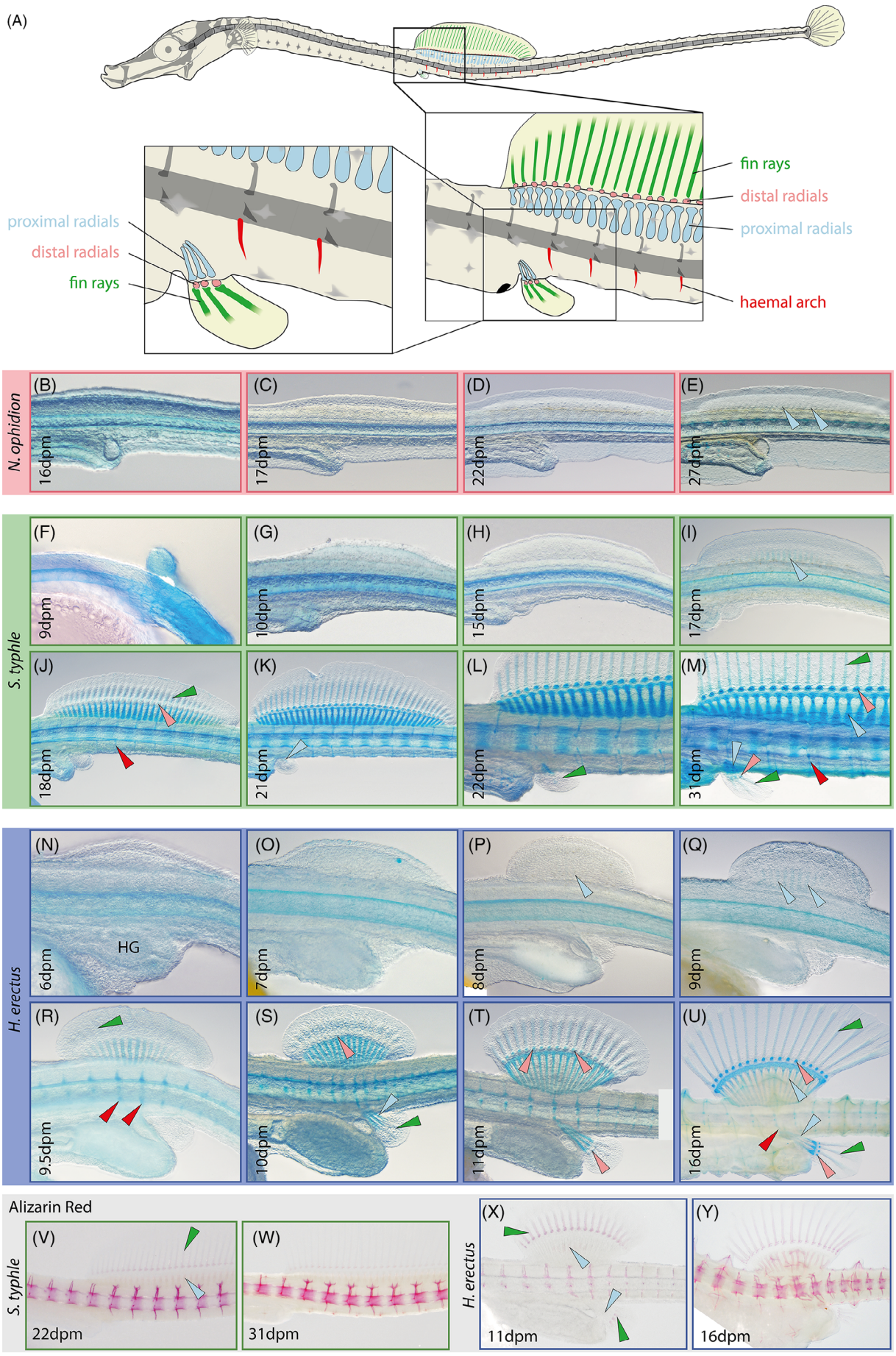

FIGURE 18 Legend on next page.

Anlage can be detected during development (15-19 dpm), which possibly corresponds to a rudimentary uroneural (pink arrowhead in Figure 19L). In *H. erectus*, the caudal fin is degenerated (as reported before for other *Hippocampus*[17,19,50]) and although some hypural cartilage is formed (10 dpm; blue arrowhead in Figure 19T), it does not attain a shape resembling the caudal fin in *S. typhle* (Figure 19T-Z). The outgrowth of two to five developing rays, as suggested by actinotrichia, stagnates soon after its onset and these are not recognizable anymore in adult *H. erectus* (green arrowheads in Figure 19V-Z; see also in situ hybridization section below).

Ossification in the most posterior spine region of *N. ophidion* was only detected in subadult fish, with seemingly uniform vertebrae merely decreasing in size forming the caudal tip (Figure 19I) and vertebrae do not show any observable differentiation. In contrast, ossification of the hypural cartilage commences at 22 dpm in *S. typhle* (blue arrowhead in Figure 19 ii) with rays starting to ossify already 1 to 2 days earlier (green arrowheads in Figure 19 ii). In *H. erectus*, the hypural cartilage does not undergo ossification before release; however, alizarin red staining shows how the very organized patterns of one neural and hemal spine per vertebra typical for the rest of the caudal region is disrupted in the most posterior vertebrae (Figure 19 iv), likely illustrating the overall disarray of regulatory processes orchestrating the ural region's development in this species.

2.3 | *Col10a1a* reveals particularly active zones of cartilage and bone formation

Teleost *col10a1a* is expressed in differentiating chondrocytes and osteoblasts and thus in situ hybridization can reveal the developmental onset of such cartilaginous and bony skeletal structures. In the examined stages, *col10a1a* expression was first detected in the maxillary process, cleithrum, and auditory capsule (purple, orange, and rose arrowheads) revealing the presence of these structures already after 12 to 15 dpm and 7 dpm in *S. typhle* and *H. erectus*, respectively (Figure 20A-C and H, respectively), which is considerably earlier than Alcian blue staining suggested. Subsequently, *col10a1a* expression was detected in the retroarticulare, hyomandibular complex, and the frontale (light green, violet, and white arrowheads, respectively, in Figure 20; 15 to 16 dpm and 9.5 dpm in *S. typhle* and *H. erectus*, respectively). After these stages, *col10a1a* expression was primarily detected in the outgrowing fin lepidotrichia (even in the rudimentary caudal fin of *H. erectus*; Figure 20M-O; green arrowheads), and while in *S. typhle*, col10a1a expression in caudal and dorsal fin rays preceded those of the pectoral and anal fins by several days (Figure 20F and G; green arrowheads), onset of *col10a1a* expression in all fin rays of *H. erectus* was more synchronized (Figure 20M-O; green arrowheads). Finally, considerable *col10a1a* expression was also detected in the seahorse's anterior portion of the snout at 14 dpm (most notably in the dentary and premaxilla; blue and dark green arrowheads, respectively; Figure 20O), the cerato- and hypohyal (violet arrowheads; Figure 20O) and also in the center of emerging bony plates in *H. erectus* (black arrowheads, Figure 20O).

2.4 | Myogenesis in syngnathids as revealed by *in situ* hybridization

Seahorse skeletal musculature has been investigated in conjunction with the fish's unique grasping tail in previous studies.[45,51] We investigated the early development of such muscle using in situ hybridization for *mybpc1*, a gene expressed in slow striated skeletal muscle[52] that proved to be a useful marker gene for all skeletal muscle in this study (see also Section 5; Figure 21). Notably, less distinct and pronounced gene expression patterns in *N. ophidion* suggest a nonoptimal in situ hybridization in this species and more subtle expression patterns were likely missed (e.g., head musculature).

Patterns of skeletal myogenesis are similar across examined species and commences with the axial musculature and myomeres form adjacent to the somites (blue arrowheads; present at 14, 10, and 4 dpm [and potentially before], in *N. ophidion*, *S. typhle*, and *H. erectus*, respectively; Figure 21A,E,K). Soon after expression patterns of *mybpc1* also suggest that axial musculature is separated into the epaxial and hypaxial portion, which will be separated by the transversal process upon its formation (dark and light blue arrowheads, respectively; present at 17, 15, and 7 dpm, in *N. ophidion*, *S. typhle*, and *H. erectus*, respectively; Figure 21B,G,L). At the same stage,

FIGURE 18 Dorsal, anal fin, and hemal arch skeletal development in examined syngnathids. (A) Main skeletal structures contributing to the dorsal and anal fin, and posterior axial skeletal elements in juvenile *Syngnathus typhle*. (B-Y) Prerelease development of the dorsal and anal fin and the posterior axial skeleton as revealed by (B-U) Alcian blue and (V-Y) Alizarin red staining. (B-E) *Nerophis ophidion*; (F-M, V, W) *S. typhle*; and (N-U, X, Y) *Hippocampus erectus*. *N. ophidion* did not show any Alizarin red staining in this region before hatching. Arrowheads: red = hemal arch/spines, green = fin rays, rose = distal radials, blue = proximal radials; dpm = days post mating

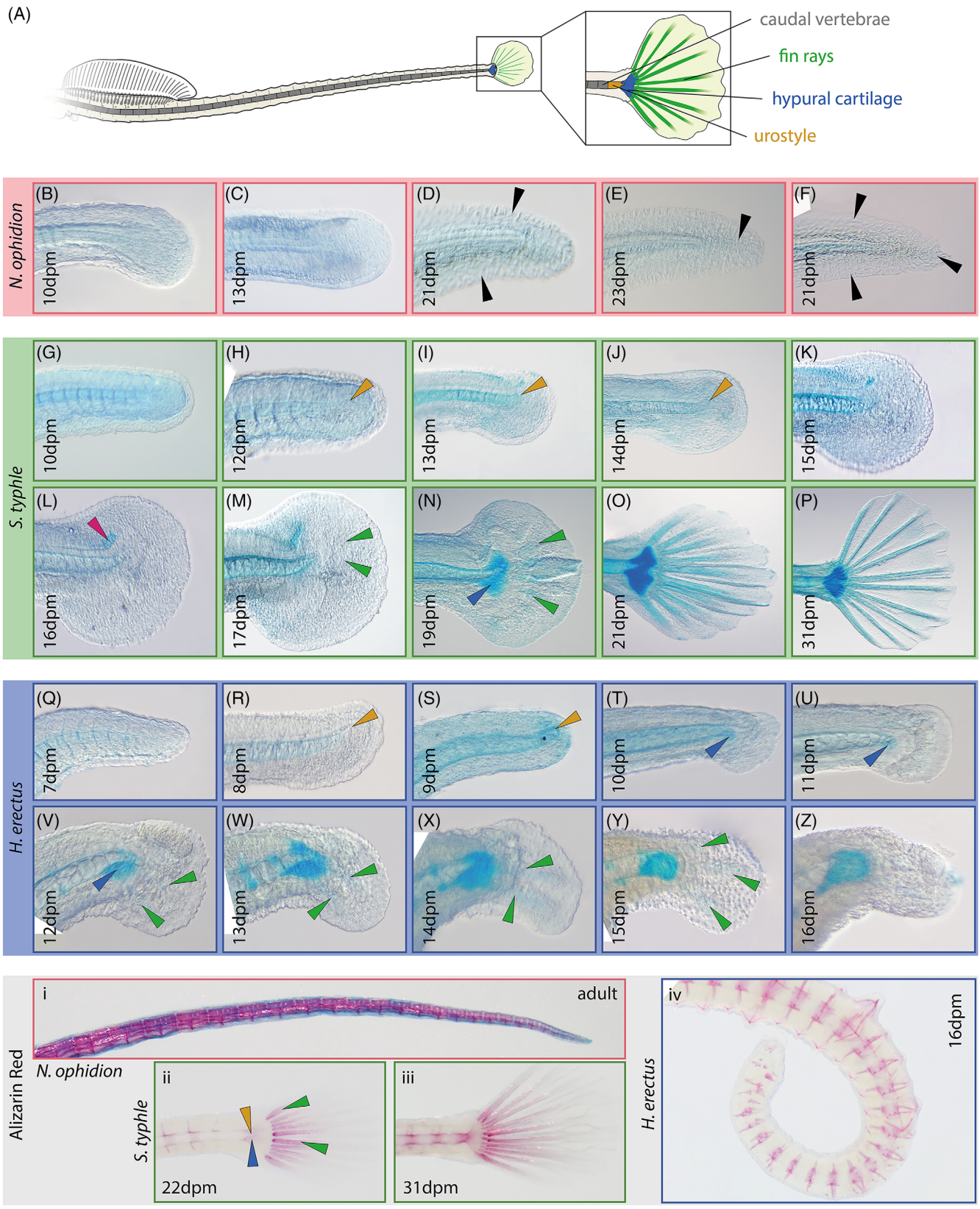

FIGURE 19 Ural region prenatal skeletal development in examined Syngnathids. (A) Main skeletal structures contributing to the ural region and caudal fin in juvenile *Syngnathus typhle*. (B-Z, i-iv) Prerelease development of the ural region and caudal fin skeleton as revealed by (B-Z) Alcian blue and (i-iv) Alizarin red staining. Arrowheads: black = fin fold, green = fin rays, ochre = urostyle, pink = alleged uroneural, blue = hypural cartilage; dpm = days post mating

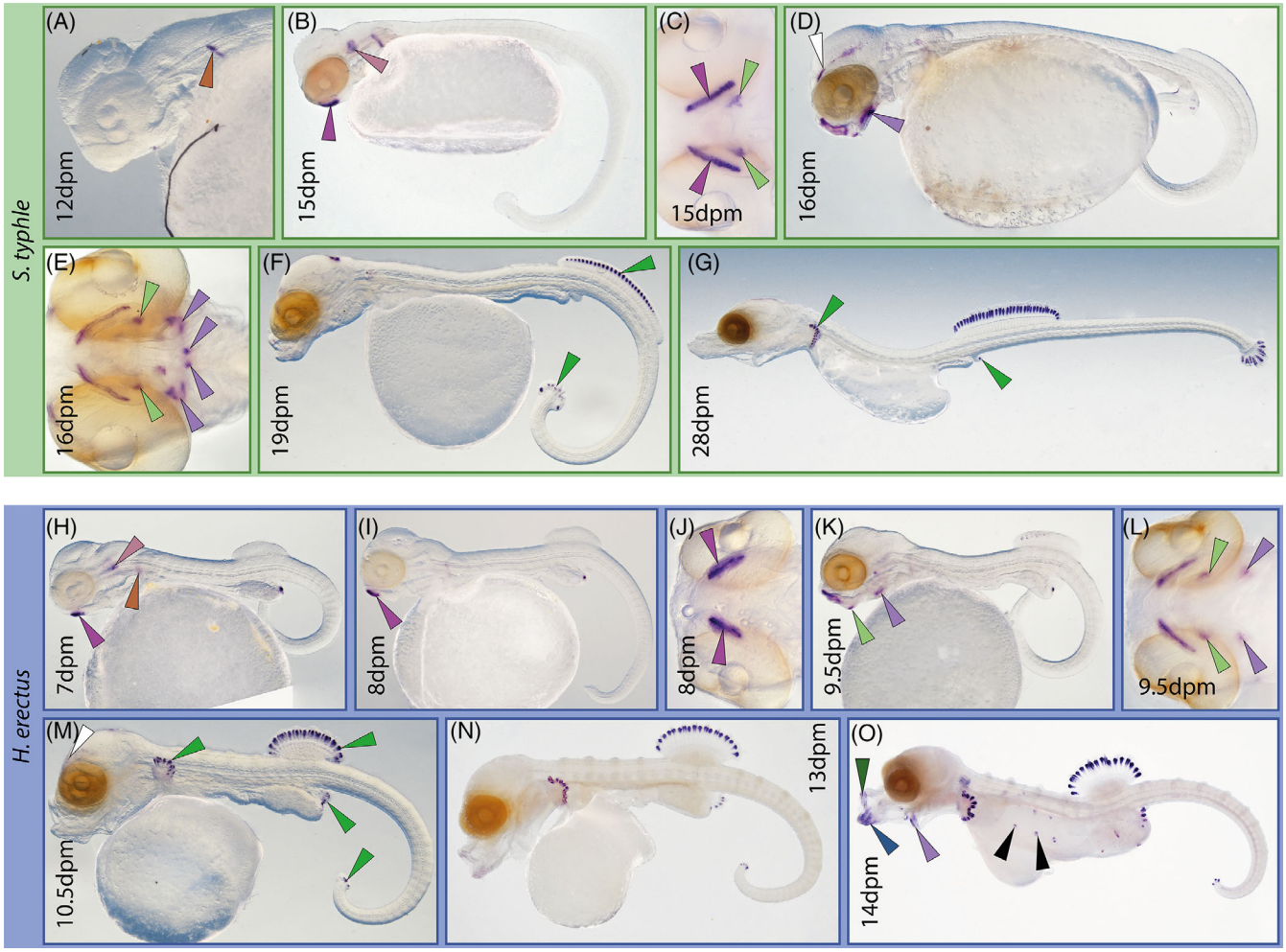

FIGURE 20 Skeletogenesis in two examined syngnathids as revealed via *col10a1a* in situ hybridization. Onset of cartilage/bone formation in (A-G) *Syngnathus typhle* and (H-O) *Hippocampus erectus*, respectively. All lateral view, except (C, E, J, L), which are ventral view. Expression of c*ol10a1a* suggests chondro-skeletogenesis commences in the pectoral girdle, followed by jaws and fin rays. Arrowheads: rose = auditory capsule, orange = cleithrum, light green = retroarticulare, green = fin rays, dark green = premaxilla, violet = hyomandibular complex, blue = dentary, white = frontale; dpm = days post mating

pronounced *mybpc1* expression outlines the sternohyoideus muscle (red arrowheads) in all species, as well as the onset of myogenesis of branchial (purple arrowheads), extraocular (cyan arrowheads), and mandibular/hyoid/hypobranchial musculature (green arrowheads in Figure 21G,L, in *S. typhle* and *H. erectus*, respectively).[9] Gene expression suggests continuous head musculature formation throughout the next few days (Figure 21H-I and M-N, in *S. typhle* and *H. erectus*, respectively). During this period, expression patterns in the axial musculature become more differentiated, suggesting an earlier conclusion of myogenesis of epaxial compared to hypaxial musculature in the trunk (with the exception of the myomeres directly associated to the dorsal fin, where *mybpc1* expression can remain strong possibly due to the formation of additional muscles orchestrating this fin's movements; Figure 21B-C; H-I; L-N, in *N. ophidion*, *S. typhle*, and *H. erectus*, respectively). In the caudal region, *mybpc1* expression attenuates first anteriorly, with posterior myomeres retaining higher expression levels, which likely reflects their later onset of development. In late embryonic stages, *mybpc1* expression is only detected in ventral trunk musculature that is likely involved in the closure of the body wall once the yolk sack is sufficiently resorbed during the last days before release, but the identity of this musculature is unclear (rose arrowheads in Figure 21I-J,O, in *S. typhle* and *H. erectus*, respectively). When larvae/juveniles are released, distinct *mybpc1* expression could not be detected anymore (data not shown), arguing for a conclusion of myogenesis onset prior to this event. The less distinct *mybpc1* expression patterns in *N. ophidion* suggest a similar myogenesis pattern to *S. typhle*, but again with a substantial delay in relative prenatal timing, as, for

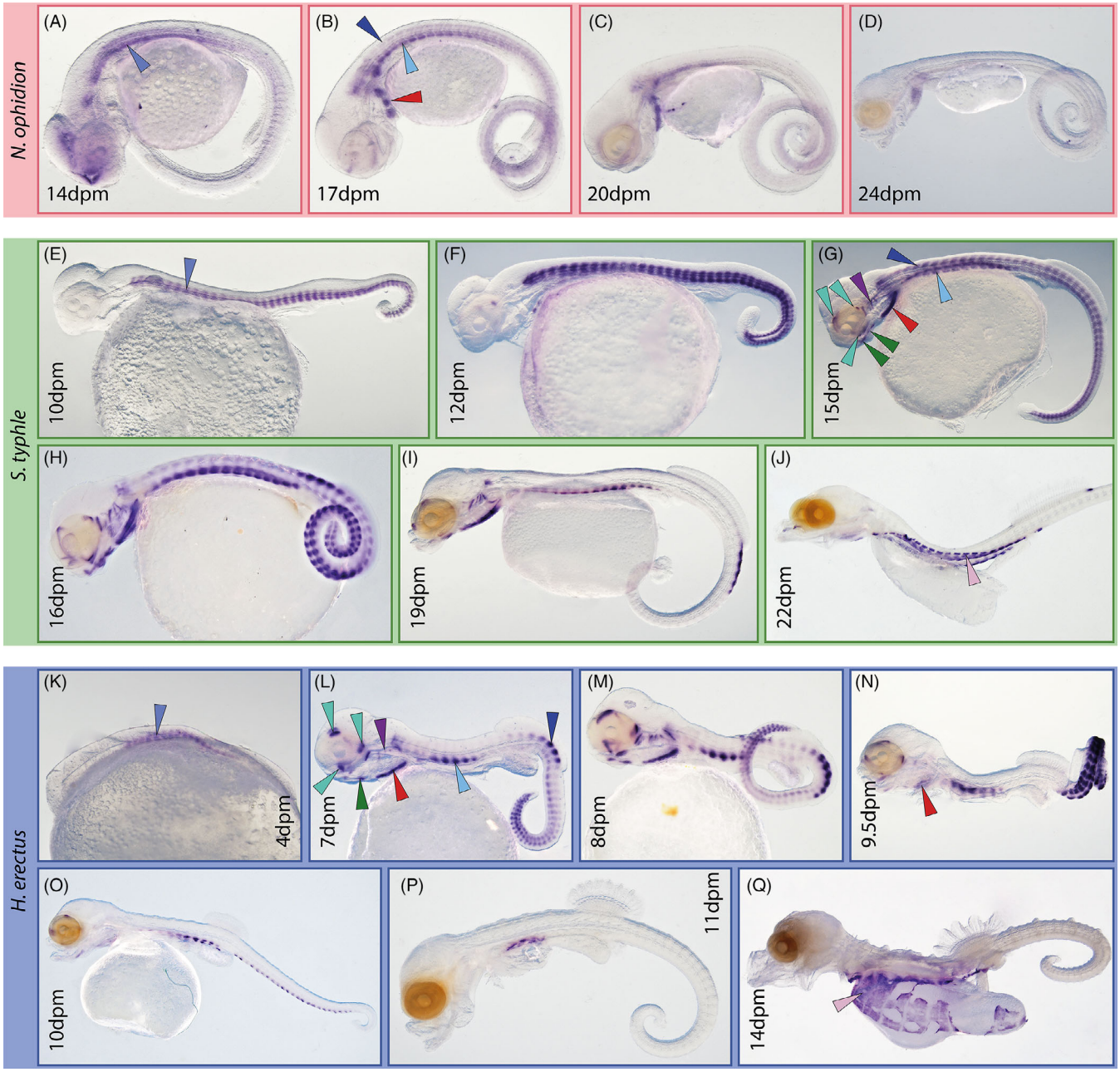

FIGURE 21 Formation of slow skeletal muscle in examined syngnathids as revealed via *mybpc1* in situ hybridization. Skeletal muscle formation in (A-D) *Nerophis ophidion*, (E-J) *Syngnathus typhle*, and (K-Q) *Hippocampus erectus*, respectively. *Mybpc1* expression suggests that myogenesis commences with axial musculature and epaxial and hypaxial expression patterns vary between species. Head musculature follows and appears to be concluded before release. All lateral view; in (K) head is missing. Arrowheads: blue = myomeres, light blue = hypaxial myomeres, dark blue = epaxial myomeres, red = sternohyoideus muscle, purple = branchial musculature, cyan = extraocular musculature, green = mandibular/hyoid/hypobranchial musculature, rose = ventral trunk musculature; dpm = days post mating

instance, the *mybpc1* expression patterns of *N. ophidion* at 24 dpm (Figure 21D; approx. 89% of prenatal development concluded) corresponds to a stage found at 22 dpm in *S. typhle* (Figure 21J; approx. 71% of prerelease development concluded).

3 | DISCUSSION

Syngnathids are extremely derived fishes featuring some of the most bizarre phenotypes found in teleosts, such as their fin loss, very unusual body shapes, paternal care and highly

modified immune systems.[6-8] Many of these iconic traits develop before the embryos hatch (or are born) and thus only few studies have so far attempted to describe the developmental trajectory turning a seemingly generic fish embryo into an evolutionary extravaganza.

3.1 | Comparative development of studied syngnathids: Direct vs indirect development

Studied syngnathids' exhibit quite distinct adult morphologies: *N. ophidion* being extremely elongated with a small head and almost no fins, *S. typhle* with a more generic pipefish body morphology, and *H. erectus* with the upright posture of the seahorses (Figure 1). During development, however, the smaller evolutionary distance and possibly the more similar mode of parental care between *S. typhle* and *H. erectus* becomes apparent,[28,53] as their development is more synchronized and more pronounced differences between the two appear relatively late in development (Figure 2). Both species also have a rather direct development, with juveniles released during birth relatively closely resembling their adult forms, and all characteristic body features (such as the adult set of fins and approximate body proportions) have been (or are being) developed. This stands in stark contrast to *N. ophidion*, which appears to hatch in a less developed state compared to *S. typhle*, that has a similarly long prenatal period (Figure 2). Furthermore, freshly hatched *N. ophidion* do not feature the characteristic adult traits: the head is still relatively large with a long snout (Figure 12A,B), pectoral fins are still present (Figure 12A-F) and a well-developed fin fold is used for locomotion. Instead, adult characteristics are slowly developed approximately 2 to 6 weeks after hatching (Figure 12G). Therefore, *N. ophidion* presents itself as an indirect developing species with a pronounced larval stage, while the development of *S. typhle* and *H. erectus* is much more direct, possibly as a result or by-product of their more derived form of male pregnancy.[5,6,14] Thus, developmental stage upon release may be linked to the lineage (with *Nerophinae* featuring a larval stage and *Syngnathinae* not), pregnancy type (with *Nerophis* likely not providing nutrients to embryos, while this is more likely/shown for [some] Syngnathinae[54,55]), or other factors not considered here and /or their interactions.

3.2 | Development of characteristic syngnathid traits

The snout-like jaws of syngnathids are among their most characteristic traits. We find that the onset of snout elongation is primarily driven by the elongation of the hyosymplectic cartilages and the unfolding of the ethmoid cartilage (which arises in a curved configuration) during the second half of prenatal development, and thus prior to the onset of ossification of these elements (Figures 8-10). By rotation/remodeling of the palatoquadrate to an almost perpendicular position to the hyosymplectic the tube-like buccal cavity is formed (Figure 11B-D), which crucially facilitates pivot feeding.

Bony dermal plates are another characteristic of syngnathids that is also found in other fish families, such as sticklebacks, and while the homology of plates across these clades was never established, their occurrence contributed to their (no longer accepted) grouping into the Gasterosteiformes.[56] Here, we find that syngnathid bony plates arise from cross-like tissue condensations late in prenatal development (Figures 13 and 14). As we observed that—within each plate row—per vertebra exactly one bony plate is formed, we infer that their ontogeny is closely linked to the segmented trunk as provided by the somites.[14] Yet, the exact homology of bony plates across fishes, and/or whether evolutionarily available gene networks were co-opted during their evolution, remains unknown. Furthermore, it remains unclear what determines the number of plate rows along the trunk and tail region of the fish. Finally, as plates show a variety of different joint types, exploring the mechanisms determining which joint type forms during development, and understanding if these joint types are genetically predetermined or if joint development is (partially) informed by mechanical interactions among neighboring plates during development, would further our understanding of how complex novel morphological structures can evolve.

Among syngnathids, the presence or absence of fins appears to be a particularly diverse characteristic and for any single fin that is found among syngnathids (e.g., the fin set that *S. typhle* has) there are representatives that have lost that particular fin (or multiple). For instance, in *N. ophidion*, we did not identify any evidence of a (rudimentary) caudal fin being formed even early on in development, suggesting that the regulatory molecular network underlying caudal fin formation (or in fact the whole ural region; Figure 19B-F,I) is dysfunctional at an upstream position, leading to a complete fin loss (similar to pelvic fin loss across all syngnathids[8]; Figure 19). In contrast, in *H. erectus*, we (as many before, e.g., [17,19,50]) have observed the onset of fin development while generic fin differentiation and outgrowth failed, arguing for a downstream dysfunction that led to a functional fin loss.

Another example of fin loss could again be observed in the indirectly developing *N. ophidion*, where larval pectoral fins are lost during the metamorphosis several weeks after hatching. In these fish, pectoral fins and a

well-developed median fin fold along the tail are resorbed (and also the head shape changes, for example, the snout becomes shorter; Figures 12 and 16). A similar, but even more extreme metamorphosis has been described before in *Bulbonaricus brucei* (pug-nosed pipefish),[57] in which even the larval dorsal fin is resorbed (and facial alterations are more extreme, leading to a pug-like facial appearance). Our study reveals that in *N. ophidion*'s generic pectoral fin development was never actually concluded, despite the pectoral fins are used by the larvae during their first weeks post hatching. Instead, pectoral fin development was seemingly truncated before skeletal differentiation occurred, and while fin outgrowth in size continued, the fin morphology clearly remained neotenic (Figure 17A-D). Similar to the caudal fin loss in *H. erectus*, this argues for a rather downstream dysfunction in the generic pectoral fin regulatory network. Such patterns of aborted development resembles digit loss in cows or birds where the Anlagen of the missing digit are specified during embryogenesis but fail to develop into a lasting adult structure.[58,59] Exploring evolutionary shifts in musculoskeletal allometric growth patterns (e.g., via heterochrony) might thus be a fruitful approach to understand the evolutionary trajectories underlying some of the most iconic syngnathid traits, such as the prehensile tail or craniofacial differences (as suggested in Reference 19). Finally, another interesting avenue for further research is to understand how metamorphosis induces the substantial developmental remodeling observed in maturing *N. ophidion* (and more so in pugnose pipefish) and identify (hormonal) triggers, such as thyroid hormone,[60,61] leading and controlling this process. Hormones have been shown to be instrumental in governing the metamorphosis of larval characters, such as the absence of fin rays in certain fins, into their adult phenotypes in numerous teleost fishes (and amphibians[62]).[61,63-67] Furthermore, subtle experimental modifications of hormone levels have been shown to generate neotenic adults,[56,68,69] and thus it is plausible that also evolution can act on endocrine signaling. Evolutionary tinkering with endocrine signaling leading to various forms of heterochrony may thus be one of the main sources of morphological variation across syngnathids.[68,69]

3.3 | Are seahorses developmentally truncated pipefish?

An important derived feature of seahorses is their characteristic upright swimming position, whereby their trunk is oriented vertically, while the head is oriented not upright but horizontally (or even more bend toward the trunk; Figure 1D). This bend posture, with the snout at a sharp angle to the trunk, can be observed early during ontogeny, around 11 dpm (Figure 5J). Although the swimming posture of pipefishes is typically horizontal and their head and trunk are aligned, they pass through a seahorse-like developmental stage (e.g., *S typhle* 21 dpm; Figure 5E) during which head and trunk form a 90° angle. This would suggest homologous body plan postures during development but a failure of seahorses to complete the process of straightening their head-trunk connection, that is, developmental truncation of an ancestral ontogenetic trajectory. As discussed before, another potential indication for developmental truncation during seahorse development as compared to their sister pipefish clade (here: *S. typhle*) is the abortion of caudal fin development (Figure 19Q-Z). In the latter case, it is clear that an Anlage forms which proceeds till the stage of fin ray condensations (as shown by *col10a1a* in situ hybridization; Figure 20M). The outgrowth is, however, precociously terminated leading to the absence of caudal fins in adults. Therefore, our ontogenetic comparison between *H. erectus* and *S. typhle* development provides several indications that the unique body plan of seahorses could in part result from developmental truncation.

4 | CONCLUDING REMARKS

Syngnathids feature some of the most bizarre traits found among fish, such as bony plates, snout-like facial anatomy, male pregnancy, highly modified immune systems, and many others.[5,7,8,45] For some of these traits, understanding the developmental trajectories syngnathids undergo is vital to unravel the evolutionary mechanisms and ecological and life-history events affecting trait development. Our study provided such insights and despite of being focused on primarily the early life development of few selected syngnathids, we recognized in our data a plethora of potential evolutionary mechanisms shaping specific aspects of syngnathid evolution and development, and believe that particularly heterochrony may be underlying some of the morphological variability found in this extraordinarily diverse family of fish.

5 | EXPERIMENTAL PROCEDURES

5.1 | Fish husbandry and sample collection

Fish used in this study were kept at the fish keeping facilities of the Helmholtz-Centre for Ocean Research Kiel

(GEOMAR). Pipefishes were originally collected in a shallow, close-by eelgrass meadow; coordinates: 54.391103, 10.191419; seahorses were obtained from commercial fish breeders, and sampling occurred from March to August 2020. *N. ophidion* and *S. typhle* stock individuals were kept in community tanks at 16°C to 18°C and *H. erectus* at 23°C (all ±0.5°C) and inspected daily for pregnancies. When a pregnancy was detected, for *N. ophidion* and *S. typhle* the individual was separated and kept at constant 16°C in a smaller tank connected to a water circulation system, while *H. erectus* were kept in their stock tanks as individuals could easily be identified. *S. typhle* and *H. erectus* were fed live and dead mysids, while *N. ophidion* received live *Artemia* nauplii and live mysids, and all food was enriched with vitamins and fatty acids. Measurements taken in this study reflect individuals kept and raised at these temperatures and developmental times may differ when fish are raised at other temperatures (temperature affects developmental speed[70,71]).

For sampling, pregnant *S. typhle* and *H. erectus* individuals were killed using MS222 and subsequently decapitated. The brooding flaps/pouch were opened and eggs/larvae were removed. For *N. ophidion*, eggs could easily be removed from the fathers' bellies using brushes, and males could be sampled several times in this manner, providing a continuous series of eggs with a known age difference. Obtained eggs were dechorionated and embryos were either immediately killed using MS222, photographed and fixed (using 4% PFA in PBS, overnight, and then gradually moved to MeOH; some photos were taken post fixation and MeOH storage) or, in the case of selected *H. erectus* embryos, cultivated in vitro in petri dishes at the same temperature as their parents until sampling. Note that the size of the yolk sac prior to full gastrulation was affected by the osmolarity of the water in which the eggs were submerged for photography (filtered Baltic sea water of ~17 ppm). Culturing *H. erectus* embryos was challenging and always led to some losses, especially when early stages (before ~50%-60% of development was concluded) were used. In our trials, filtered North Sea seawater diluted to a salinity of ~20 ppm was used, as embryos (age 1-7 days) showed highest average survival at this salinity. For embryos older than 12 days, salinity was gradually increased to meet 35 ppm after 16 days. As mating could only be observed for few *H. erectus* individuals during this experiment, intermediate stages were obtained by rearing offspring in vitro, as described, and daily sampled. In *H. erectus*, while stages for each day in development were identified, they likely not represent 24 hours intervals each time (e.g., day 9 to 10, and 10 to 11 are likely >24 hours), possibly due to slightly slower growth rates of embryos in vitro and because the onset of embryonic development was never exactly known, as fertilization occurs inside the pouch. Therefore, the manuscript uses the unconventional "hours/days post mating" (dpm) to indicate the age of embryos. While in many teleosts, the time of mating and fertilization coincides, in syngnathids this is likely not the case and fertilization happens some time (potentially hours) after mating concealed from the observer within the brooding organ.

5.2 | Skeletal staining procedures, imaging of embryos, and morphological annotation

Skeletal stains were performed on fixed embryos/larvae using the following staining solution (for 1 mL of "low-acid double-stain"): 12.5 µL Alcian blue solution (0.4% in 70% EtOH), 50 µL acetic acid (100%), 57.5 µL $MgCl_2$ (2 M), 870 µL EtOH (70%), 10 µL Alizarin red solution (0.5% in H_2O), based on Reference 43. Stains were performed typically for 3 to 4 hours, but larger individuals (i.e., free-swimming larvae, juveniles, adults) were kept for up to 12 hours in staining solution. Treating embryos for even 15 to 20 minutes in the low-acid staining solution dissolved all subtly ossified structures and led to a delayed detection of mineralization (very labile mineralizing was already noted by Azzarello[25] for syngnathids), and additional Alizarin red staining did not recover these patterns, but only led to strongly stained yolk sacs (see Figure 6L). Also, as acid-free double staining solution (according to Reference 43) did not yield skeletal double-stains of sufficient quality even after optimization, staining for Alizarin red was performed (10 µL Alizarin red solution [0.5% Alizarin red in H_2O] per milliliter 70% EtOH) on separate individuals. After staining, individuals were repeatedly washed in 70% EtOH, gradually transferred to H_2O, and then bleached and cleared using 0.5% to 1.5% H_2O_2 in 0.5% to 1% KOH, depending on pigmentation stage for 5 to 30 min; juveniles and adults longer, and continued to be clear in 0.5% KOH in 50% glycerol for several hours to days.

Photographs of embryos were taken using a Nikon SMZ18 stereomicroscope system equipped with a DS-Fi3 camera. For positioning purposes, samples were typically photographed on agarose gels with indentations for yolk sacs or fins, facilitating the proper alignment of the embryos. In early stages, eggs were dechorionated whenever possible without damaging the embryo. Obtained photos were processed in Adobe Photoshop. The following parameters (or a subset of them) were adjusted in obtained images: brightness ("exposure") and contrast, white balance, rotation and reflection, cropping, shadows/highlights (strongly pigmented eyes appear

brighter), saturation, agarose-gel background noise removal and extension. For photos taken of fluorescent Alizarin red, background fluorescence was removed by adjusting the color curve and overlays were also produced in Photoshop. All adjustments (except for the background) were always applied to the whole image and none was made with the intention to hide/distort any information of the obtained photos. For all images, raw file copies are available upon request.

Morphological structures were identified according to previously published work.[10,17,19,20] The branchial basket could generally not be visualized well across all stages in this study and thus was not described, as it was done before in detail.[18,72,73] Measurements (e.g., ray counts, length measurements) were only recorded in one or few individuals per time point, as especially *H. erectus* samples came from fish stocks that have been kept in the lab for generations and the genetic variability of these stocks is expected to be reduced compared to natural populations, and fin meristics have been published for all three species before.[74,75] Embryo body length was measured based on lateral photos using the segmented line tool in ImageJ (v. 1.5.1) from the causal peduncle to the forehead. The "snout" region was not included as it showed particularly high variability in length even within broods and thus measurements would have been noisier. Logistic regression fit lines were fitted using the nls() function in R (v. 4.1.3).[76]

5.3 | Geometric morphometric analysis

Forty four landmarks identified in ImageJ on lateral photos of heads were used to describe the shape of syngnathid heads and its key cartilages across developmental stages (photos across species and stages were randomized for this process; *N. ophidion* = 29, *S. typhle* = 42; *H. erectus* = 49; Figure 11A; Supplementary Table S1). As structures were not always identifiable/unambiguous at all stages, landmark locations were estimated when structures were not visible (i.e., not yet developed). This was necessary as the PCA, which was employed for data analysis, requires a complete set of landmarks across all samples. Furthermore, several landmarks were put along a smooth structure contour (e.g., to describe the ethmoid cartilage bending, Figure 11A) and thus cannot be considered taxic homolog, but instead they were put approximately with equal distance to one another on the respective structure. This approach led in our evaluation to more accurate representation of shape homology when compared to treating the landmarks as sliding (semi-) landmarks. Due to these limitations, the geometric morphometric dataset was interpreted cautiously. A generalized Procrustes analysis was performed on obtained datapoints (gpagen() function from "geomorph" package v. 4.1.2[77]) and a PCA was conducted in R (v. 4.1.3).[76] A scree-plot suggested that most variation is loaded on PC1-3 (PC4 explains ~2.3% of variation and is not considered here anymore).

5.4 | In situ hybridization procedures

In situ hybridization was performed to visualize the expression of *col10a1a* and *mybpc1* to monitor cartilage/bone and skeletal muscle formation, respectively.[78,79] *Col10a1a* is in teleosts expressed both in differentiating chondrocytes and osteoblasts expression expressed,[78] and facilitates the detection of especially bone formation much earlier than staining techniques used in the manuscript. Thus, the two approaches complement each other. *Mybpc1* was described to be expressed in slow striated skeletal muscle[80] but proved in this study to be a useful marker gene using in situ analysis for overall early skeletal muscle development as it revealed distinct and unambiguous patterns. As gene trees confirmed that indeed *mybpc1* (and not its paralogs) was cloned to synthesize in situ probes, observed expression patterns suggest that *mybpc1* is also expressed in fast striated muscle development in syngnathids.

AUTHOR CONTRIBUTIONS

Ralf Friedrich Schneider: Conceptualization (equal); data curation (lead); formal analysis (lead); investigation (lead); methodology (lead); project administration (equal); resources (lead); software (lead); visualization (lead); writing – original draft (lead); writing – review and editing (equal). **Joost M. Woltering:** Conceptualization (equal); investigation (equal); methodology (equal); supervision (equal); visualization (equal); writing – review and editing (lead). **Dominique Adriaens:** Conceptualization (equal); methodology (equal); supervision (equal); writing – review and editing (equal). **Olivia Roth:** Conceptualization (equal); funding acquisition (lead); methodology (equal); project administration (equal); resources (equal); supervision (lead); writing – review and editing (equal).

ACKNOWLEDGMENTS

The authors would like to thank Fabian Wendt for raising *N. ophidion* larvae, Beke Hansen for preliminary work on the geometric morphometrics dataset and Katharina Krüger for helping with skeletal stainings and their photography. This project was supported by the European Research Council (ERC) under the European Union's Horizon Research and Innovation Program (MALEPREG: eu-repo/grantAgreement/EC/H2020/

755659) to O. R. Deutsche Forschungs Gemeinschaft (DFG) to J. M. W. (WO-2165/2-1 and WO-2165/2-2). Open Access funding enabled and organized by Projekt DEAL.

CONFLICT OF INTEREST

The authors declare no potential conflict of interest.

DATA AVAILABILITY STATEMENT

Geometric morphometric measurements can be found in the Supplementary Data.

ETHICS STATEMENT

All experiments were conducted in accordance with local ethics regulations (University of Kiel Anzeige §4 1315).

ORCID

Ralf F. Schneider https://orcid.org/0000-0001-6015-7219
Joost M. Woltering https://orcid.org/0000-0002-2630-6572
Dominique Adriaens https://orcid.org/0000-0003-3610-2773
Olivia Roth https://orcid.org/0000-0002-7349-7797

REFERENCES

1. Small C, Bassham S, Catchen J, et al. The genome of the Gulf pipefish enables understanding of evolutionary innovations. *Genome Biol*. 2016;17(1):258.
2. Small CM, Healey HM, Currey MC, et al. Leafy and weedy seadragon genomes connect genic and repetitive DNA features to the extravagant biology of syngnathid fishes. *Proc Natl Acad Sci U S A*. 2022;119(26):e2119602119.
3. Qu M, Liu Y, Zhang Y, et al. Seadragon genome analysis provides insights into its phenotype and sex determination locus. *Sci Adv*. 2021;7(34):eabg5196.
4. Teske PR, Beheregaray LB. Evolution of seahorses' upright posture was linked to Oligocene expansion of seagrass habitats. *Biol Lett*. 2009;5(4):521-523.
5. Stölting KN, Wilson AB. Male pregnancy in seahorses and pipefish: beyond the mammalian model. *Bioessays*. 2007;29(9):884-896.
6. Wilson AB, Vincent A, Ahnesjö I, Meyer A. Male pregnancy in seahorses and pipefishes (family Syngnathidae): rapid diversification of paternal brood pouch morphology inferred from a molecular phylogeny. *J Hered*. 2001;92(2):159-166.
7. Roth O, Solbakken MH, Tørresen OK, et al. Evolution of male pregnancy associated with remodelling of canonical vertebrate immunity in seahorses and pipefishes. *Proc Natl Acad Sci U S A*. 2020;117:9431-9439.
8. Lin Q, Fan S, Zhang Y, et al. The seahorse genome and the evolution of its specialized morphology. *Nature*. 2016;540(7633):395-399.
9. Van Wassenbergh S, Roos G, Genbrugge A, et al. Suction is kid's play: extremely fast suction in newborn seahorses. *Biol Lett*. 2009;5(2):200-203.
10. Leysen H, Jouk P, Brunain M, Christiaens J, Adriaens D. Cranial architecture of tube-snouted gasterosteiformes (*Syngnathus rostellatus* and *Hippocampus capensis*). *J Morphol*. 2010;271(3):255-270.
11. Praet T, Adriaens D, Cauter SV, Masschaele B, Beule MD, Verhegghe B. Inspiration from nature: dynamic modelling of the musculoskeletal structure of the seahorse tail. *Int J Numer Method Biomed Eng*. 2012;28(10):1028-1042.
12. Porter MM, Novitskaya E, Castro-Ceseña AB, Meyers MA, McKittrick J. Highly deformable bones: unusual deformation mechanisms of seahorse armor. *Acta Biomater*. 2013;9(6):6763-6770.
13. Wilson AB, Ahnesjo I, Vincent AC, Meyer A. The dynamics of male brooding, mating patterns, and sex roles in pipefishes and seahorses (family Syngnathidae). *Evolution*. 2003;57(6):1374-1386.
14. Woltering JM, Holzem M, Schneider RF, Nanos V, Meyer A. The skeletal ontogeny of *Astatotilapia burtoni*—a direct-developing model system for the evolution and development of the teleost body plan. *BMC Dev Biol*. 2018;18(1):1-23.
15. Flegler-Balon C. Direct and indirect development in fishes—examples of alternative life-history styles. *Alternative Life-History Styles of Animals*. Kluwer AcademicPublisher, Dordrecht, The Netherlands; 1989:71-100.
16. Balon EK. Alternative ways to become a juvenile or a definitive phenotype (and on some persisting linguistic offenses). *Environ Biol Fishes*. 1999;56(1):17-38.
17. Novelli B, Otero-Ferrer F, Socorro J, Caballero M, Segade-Botella A, Domínguez LM. Development of short-snouted seahorse (*Hippocampus hippocampus*, L. 1758): osteological and morphological aspects. *Fish Physiol Biochem*. 2017;43(3):833-848.
18. Novelli B, Socorro J, Caballero M, Otero-Ferrer F, Segade-Botella A, Molina DL. Development of seahorse (*Hippocampus reidi*, Ginsburg 1933): histological and histochemical study. *Fish Physiol Biochem*. 2015;41(5):1233-1251.
19. Franz-Odendaal TA, Adriaens D. Comparative developmental osteology of the seahorse skeleton reveals heterochrony amongst Hippocampus sp. and progressive caudal fin loss. *Evo-Devo*. 2014;5(1):1-12.
20. Kadam K. The development of the chondrocranium in the seahorse, Hippocampus [Lophobranchii]. *Zool J Linn Soc*. 1958;43(293):557-573.
21. Sommer S, Whittington CM, Wilson AB. Standardised classification of pre-release development in male-brooding pipefish, seahorses, and seadragons (family Syngnathidae). *BMC Dev Biol*. 2012;12(1):1-6.
22. Wetzel JT, Wourms JP. Embryogenesis in the dwarf seahorse, Hippocampus zosterae (Syngnathidae). *Gulf Caribb Res*. 2004;16(1):27-35.
23. Mi PT, Kornienko E, Drozdov A. Embryonic and larval development of the seahorse Hippocampus kuda. *Russ J Mar Biol*. 1998;24(5):325-329.
24. Kornienko E. Reproduction and development in some genera of pipefish and seahorses of the family Syngnathidae. *Russ J Mar Biol*. 2001;27(1):S15-S26.
25. Azzarello MY. A comparative study of the developmental osteology of *Syngnathus scovelli* and *Hippocampus zosterae* (Pisces, Syngnathidae) and its phylogenetic implications. *Evol Monogr*. 1990;12.

26. Maters BR, Stevenson E, Vize PD. Embryonic and aglomerular kidney development in the bay pipefish, *Syngnathus leptorhynchus*, *bioRxiv*. 2021.
27. Froese R, Pauly D. FishBase. *World Wide Web Electronic Publication*; 2022.
28. Hamilton H, Saarman N, Short G, et al. Molecular phylogeny and patterns of diversification in Syngnathid fishes. *Mol Phylogenet Evol*. 2017;107:388-403.
29. Longo SJ, Faircloth BC, Meyer A, Westneat MW, Alfaro ME, Wainwright PC. Phylogenomic analysis of a rapid radiation of misfit fishes (Syngnathiformes) using ultraconserved elements. *Mol Phylogenet Evol*. 2017;113:33-48.
30. Rabosky DL, Chang J, Cowman PF, et al. An inverse latitudinal gradient in speciation rate for marine fishes. *Nature*. 2018; 559(7714):392-395.
31. Li C, Olave M, Hou Y, et al. Genome sequences reveal global dispersal routes and suggest convergent genetic adaptations in seahorse evolution. *Nat Commun*. 2021;12(1094). doi:10.1038/s41467-021-21379-x
32. Braga Goncalves I, Ahnesjö I, Kvarnemo C. The relationship between female body size and egg size in pipefishes. *J Fish Biol*. 2011;78(6):1847-1854.
33. Höch R, Schneider RF, Kickuth A, Meyer A, Woltering JM. Spiny and soft-rayed fin domains in acanthomorph fish are established through a BMP-gremlin-shh signaling network. *Proc Natl Acad Sci U S A*. 2021;118(29):e2101783118.
34. Vincent AC, Berglund A, Ahnesjö I. Reproductive ecology of five pipefish species in one eelgrass meadow. *Environ Biol Fishes*. 1995;44(4):347-361.
35. Ahnesjo I. Temperature affects male and female potential reproductive rates differently in the sex-role reversed pipefish, *Syngnathus typhle*. *Behav Ecol*. 1995;6(2):229-233.
36. Monteiro N, Almada V, Vieira M. Implications of different brood pouch structures in syngnathid reproduction. *J Mar Biol Assoc U K*. 2005;85(5):1235-1241.
37. Teixeira R, Musick JA. Reproduction and food habits of the lined seahorse, *Hippocampus erectus* (Teleostei: Syngnathidae) of Chesapeake Bay, Virginia. *Rev Bras Biol*. 2001;61:79-90.
38. Jones AG, Rosenqvist G, Berglund A, Avise JC. Mate quality influences multiple maternity in the sex-role-reversed pipefish *Syngnathus typhle*. *Oikos*. 2000;90(2):321-326.
39. Kawaguchi M, Okubo R, Harada A, et al. Morphology of brood pouch formation in the pot-bellied seahorse *Hippocampus abdominalis*. *Zool Lett*. 2017;3(1):19.
40. Kimmel CB, Ballard WW, Kimmel SR, Ullmann B, Schilling TF. Stages of embryonic development of the zebrafish. *Dev Dyn*. 1995;203(3):253-310.
41. Iwamatsu T. Stages of normal development in the medaka *Oryzias latipes*. *Mech Dev*. 2004;121(7–8):605-618.
42. Parichy DM, Elizondo MR, Mills MG, Gordon TN, Engeszer RE. Normal table of postembryonic zebrafish development: staging by externally visible anatomy of the living fish. *Dev Dyn*. 2009;238(12):2975-3015.
43. Walker M, Kimmel C. A two-color acid-free cartilage and bone stain for zebrafish larvae. *Biotech Histochem*. 2007;82(1):23-28.
44. Leysen H, Christiaens J, De Kegel B, Boone M, Van Hoorebeke L, Adriaens D. Musculoskeletal structure of the feeding system and implications of snout elongation in *Hippocampus reidi* and *Dunckerocampus dactyliophorus*. *J Fish Biol*. 2011;78(6):1799-1823.
45. Neutens C, Adriaens D, Christiaens J, et al. Grasping convergent evolution in syngnathids: a unique tale of tails. *J Anat*. 2014;224(6):710-723.
46. Lees J, Märss T, Wilson MV, Saat T, Špilev H. The sculpture and morphology of postcranial dermal armor plates and associated bones in gasterosteiforms and syngnathiforms inhabiting Estonian coastal waters. *Acta Zool*. 2012;93(4):422-435.
47. Porter MM, Adriaens D, Hatton RL, Meyers MA, McKittrick J. Why the seahorse tail is square. *Science*. 2015;349(6243): aaa6683.
48. Hawkins MB, Henke K, Harris MP. Latent developmental potential to form limb-like skeletal structures in zebrafish. *Cell*. 2021;184(4):899-911.e13.
49. Consi T, Seifert P, Triantafyllou M, Edelman E. The dorsal fin engine of the seahorse (Hippocampus sp.). *J Morphol*. 2001; 248(1):80-97.
50. Kanou K, Kohno H. Early life history of a seahorse, Hippocampus mohnikei, in Tokyo Bay, Japan. *Ichthyol Res*. 2001;48(4): 361-368.
51. Hale ME. Functional morphology of ventral tail bending and prehensile abilities of the seahorse, *Hippocampus kuda*. *J Morphol*. 1996;227(1):51-65.
52. Ackermann MA, Kontrogianni-Konstantopoulos A. Myosin binding protein-C slow: a multifaceted family of proteins with a complex expression profile in fast and slow twitch skeletal muscles. *Front Physiol*. 2013;4:391.
53. Roth O, Solbakken MH, Tørresen OK, et al. Evolution of male pregnancy associated with remodeling of canonical vertebrate immunity in seahorses and pipefishes. *Proc Natl Acad Sci U S A*. 2020;117(17):9431-9439.
54. Skalkos ZM, Van Dyke JU, Whittington CM. Paternal nutrient provisioning during male pregnancy in the seahorse *Hippocampus abdominalis*. *J Comp Physiol B*. 2020;190(5): 547-556.
55. Otero-Ferrer F, Lättekivi F, Ord J, et al. Time-critical influences of gestational diet in a seahorse model of male pregnancy. *J Exp Biol*. 2020;223(3):jeb210302.
56. Kawahara R, Miya M, Mabuchi K, et al. Interrelationships of the 11 gasterosteiform families (sticklebacks, pipefishes, and their relatives): a new perspective based on whole mitogenome sequences from 75 higher teleosts. *Mol Phylogenet Evol*. 2008; 46(1):224-236.
57. Dawson C. Bulbonaricus Herald (Pisces: Syngnathidae), a senior synonym of Enchelyocampus Dawson and Allen, with description of *Bulbonaricus brucei* n. sp. from eastern Africa. *Copeia*. 1984:565-571.
58. Lopez-Rios J, Duchesne A, Speziale D, et al. Attenuated sensing of SHH by Ptch1 underlies evolution of bovine limbs. *Nature*. 2014;511(7507):46-51.
59. Welten MC, Verbeek FJ, Meijer AH, Richardson MK. Gene expression and digit homology in the chicken embryo wing. *Evol Dev*. 2005;7(1):18-28.
60. Laudet V. The origins and evolution of vertebrate metamorphosis. *Curr Biol*. 2011;21(18):R726-R737.
61. Campinho MA. Teleost metamorphosis: the role of thyroid hormone. *Front Endocrinol*. 2019;10:383.

62. Furlow JD, Neff ES. A developmental switch induced by thyroid hormone: Xenopus laevis metamorphosis. *Trends Endocrinol Metab*. 2006;17(2):40-47.
63. Miwa S, Inui Y. Effects of various doses of thyroxine and triiodothyronine on the metamorphosis of flounder (*Paralichthys olivaceus*). *Gen Comp Endocrinol*. 1987;67(3):356-363.
64. de Jesus EGT, Toledo JD, Simpas MS. Thyroid hormones promote early metamorphosis in grouper (*Epinephelus coioides*) larvae. *Gen Comp Endocrinol*. 1998;112(1):10-16.
65. Tagawa M, Aritaki M. Production of symmetrical flatfish by controlling the timing of thyroid hormone treatment in spotted halibut *Verasper variegatus*. *Gen Comp Endocrinol*. 2005;141(2):184-189.
66. McMenamin SK, Parichy DM. Metamorphosis in teleosts. *Curr Top Dev Biol*. 2013;103:127-165.
67. Power DM, Einarsdóttir IE, Pittman K, et al. The molecular and endocrine basis of flatfish metamorphosis. *Rev Fish Sci*. 2008;16(sup1):95-111.
68. Karagic N, Härer A, Meyer A, Torres-Dowdall J. Thyroid hormone tinkering elicits integrated phenotypic changes potentially explaining rapid adaptation of color vision in cichlid fish. *Evolution*. 2022;76(4):837-845.
69. Shkil F, Smirnov S. Experimental approach to the hypotheses of heterochronic evolution in lower vertebrates. *Paleontol J*. 2015;49(14):1624-1634.
70. Monteiro N, Almada V, Vieira M. Early life history of the pipefish *Nerophis lumbriciformis* (Pisces: Syngnathidae). *J Mar Biol Assoc U K*. 2003;83(5):1179-1182.
71. Silva K, Monteiro N, Almada V, Vieira M. Early life history of *Syngnathus abaster*. *J Fish Biol*. 2006;68(1):80-86.
72. Delunardo FAC, Paulino MG, Medeiros LCC, Fernandes MN, Scherer R, Chippari-Gomes AR. Morphological and histopathological changes in seahorse (*Hippocampus reidi*) gills after exposure to the water-accommodated fraction of diesel oil. *Mar Pollut Bull*. 2020;150:110769.
73. Prein M, Kunzmann A. Structural organization of the gills in pipefish (Teleostei, Syngnathidae). *Zoomorphology*. 1987;107(3):161-168.
74. Gürkan Ş. The biometric analysis of pipefish species from Çamaltı lagoon (İzmir Bay, Aegean Sea). *EgeJFAS*. 2008;25(1):53-56.
75. Lourie SA, Pollom RA, Foster SJ. A global revision of the seahorses Hippocampus Rafinesque 1810 (Actinopterygii: Syngnathiformes): taxonomy and biogeography with recommendations for further research. *Zootaxa*. 2016;4146(1):1-66.
76. R Core Team. *R: A Language and Environment for Statistical Computing*. Vienna: R Foundation for Statistical Computing; 2013.
77. Adams DC, Otárola-Castillo E. geomorph: an R package for the collection and analysis of geometric morphometric shape data. *Methods Ecol Evol*. 2013;4(4):393-399.
78. Kim Y-I, Lee S, Jung S-H, et al. Establishment of a bone-specific col10a1: GFP transgenic zebrafish. *Mol Cells*. 2013;36(2):145-150.
79. Ha K, Buchan JG, Alvarado DM, et al. MYBPC1 mutations impair skeletal muscle function in zebrafish models of arthrogryposis. *Hum Mol Genet*. 2013;22(24):4967-4977.
80. Ochi H, Westerfield M. Lbx2 regulates formation of myofibrils. *BMC Dev Biol*. 2009;9(1):1-14.

SUPPORTING INFORMATION

Additional supporting information can be found online in the Supporting Information section at the end of this article.

How to cite this article: Schneider RF, Woltering JM, Adriaens D, Roth O. A comparative analysis of the ontogeny of syngnathids (pipefishes and seahorses) reveals how heterochrony contributed to their diversification. *Developmental Dynamics*. 2023;252(5):553-588. doi:10.1002/dvdy.551